Asian Journal of
Research in Chemistry

Abstracted in
CAB Abstracts,
Google Scholar,
EBSCO Publishing's Electronic Databases,
Indian Science Abstract.
Index Copernicus,
ProQuest Central
Indian Citation Index

www.ajrconline.org

Three New Tetraphenylphosphonium Halochromates (VI), [(C₆H₅)₄P][CrO₃X], (X= F, Cl, Br): Efficient and Mild Reagents for Oxidation of Organic Substrates

Shahriar Ghamami, Mojdeh Golzani*, Amir Lashagri
Department of Chemistry, Faculty of Science, Imam Khomeini International University, Qazvin, Iran
*Corresponding Author E-mail: **mojdeh,golzani@gmail.com**

ABSTRACT:
Tetraphenylphosphonium Fluorochromate(VI), TPPFC, Tetraphenylphosphonium Chlorochromate(VI), TPPCC and Tetraphenylphosphonium Bromochromate(VI), TPPBC are new, mild and more efficient reagents which prepared easily and used for quantitative oxidation of several organic substrates. We have found that these reagents have certain advantages over similar oxidizing agents in terms of amounts of oxidants and solvents required, easier working up and high yields. These new compounds have certain advantages over similar oxidizing agents in terms of the amount of oxidants, short reaction times, and high yields.

KEYWORDS: Chromium(VI), Tetraphenylphosphonium Fluorotrioxochromate, Tetraphenylphosphonium Chlorotrioxochromate.

INTRODUCTION:

Chromium(VI) based reagents are widely used in modern organic synthesis for the oxidation of organic substrates, in particular primary and secondary alcohols, under mild conditions. Even though, numerous oxidants for oxidation of alcohols are already reported, the growing demand for new oxidants of alcohols made us carry out the synthesis of Tetraphenylphosphonium Halochromates(VI), TPPXC. Many such reagents have been developed in recent years with some success (1), Some of the important entries in the list of reagents are quinolinium fluorochromate (QFC) (2), prolinium chlorochromate (3), caffeinilium chlorochromate (4), isoquinolinium chlorochromate (5), 2,2'-bipyridinium chlorochromate (BiPCC) (6), 2,6-dicarboxypyridinium chlorochromate (7-8), pyridinium chlorochromate (PCC) (9), pyridinium dichromate (PDC) (10), pyridinium fluorochromate (PFC) (11), pyridinium bromochromate (PBC) (12), quinolinium chlorochromate (QCC) (13). and Tetramethlammonium fluorochromate (TMAFC) (14).

We have found that these reagents have certain advantages over similar oxidizing agents in terms of amounts of oxidants and solvents required, easier working up and high yields. In these respect, we wish to report that Tetraphenylphosphonium Halochromates, (TPPXC) able oxidizes alcohols to their corresponding aldehydes and ketones, under mild conditions.

EXPERIMENTAL:

Material and instruments
CrO₃ (Merck, P.A.) and Tetraphenylphosphonium Halochromates were obtained from Fluka (Buchs, Switzerland). Solvents were purified by standard methods. Infrared spectra were recorded as KBr disks on a Shimadzu model 420 spectrophotometer. The UV/Visible measurements were made on an Uvicon model 922 spectrometer. ¹H and ¹³C NMR spectra were recorded using Bruker DRX-500 in CDCl₃ solutions. In the case of the reduced product of the oxidants, chromium was determined after oxidizing with acidic peroxodisulfate (K₂S₂O₈) solution. Department of Chemistry, OIRC, Tehran. Melting points were measured on Electrothermal 9100 melting point apparatus.

Synthesis of Tetraphenylphosphonium Fluorochromates (VI), [(C₆H₅)₄P][CrO₃F]

Synthesis of Tetraphenylphosphonium Fluorochromates (VI), $[(C_6H_5)_4P][CrO_3F]$

A 1g (10 mmol) sample of chromium (VI) oxide, CrO_3, and 9ml (20 mmol) of 40% hydrofluoric acid were added to 20 ml of water in a 100 ml polyethylene beaker with stirring. After 5-7 min the homogeneous solution was cooled to ca. 0 °C. To the resultant clear orange solution, Tetraphenylphosphonium Chloride (3.74g, 10 mmol) was added with stirring to this solution over a period of 0.5 h and stirring was continued for 0.5 h at 0 °C. The solid was washed with hexane and dried under vacuum for 1 h: $C_{24}H_{20}CrFO_3P$: Cacld. %C, 62.88; %H, 4.36. Found: %C, 64.62; %H, 4.51. IR.(KBr): 875 cm^{-1} $_1(A_1)$ or (CrO₃), 640cm^{-1} $_2(A_1)$ or (Cr-F), 947 cm^{-1} $_4(E)$ or (CrO₃) cm^{-1}. UV/Visible ^{13}C-NMR and ^{1}H-NMR were all consistent with the TPPFC structure. Electronic absorption at 450 nm, corresponding to 1a₂ 9e (= 276 M^{-1} cm^{-1}); 363 nm to 8e 9e (= 462 M^{-1} cm^{-1}); and 273 nm to 12a₁ 9e (=986 M^{-1} cm^{-1}).

Synthesis of Tetraphenylphosphonium Chlorochromates (VI), $[(C_6H_5)_4P][CrO_3Cl]$

Chromium(VI) oxide (1.0 g. 10 mmol) was dissolved in dry actonitrile (25 ml) in a beaker and was added under stirring at 0 °C. To the resultant clear orange solution, Tetraphenylphosphonium chloride (3.74 g, 10 mmol) was added under stirring over a period of 0.5 h and the stirring was continued for 0.5 h at 0 °C. The precipitated clear orange solid was isolated by filtration, washed with hexan and dried under vacuum for 1 h at room temperature. To this mixture, 30 ml CH_2Cl_2 is added. The orange organic phase is decanted and the solvent is distilled off. A reddish orange gel is separated and stored in the refrigerator. $C_{24}H_{20}ClCrO_3P$: Cacld. %C, 60.69; %H, 4.21. Found: %C, 63.02; %H, 4.40. IR (KBr): 905 cm^{-1} $v_1(A_1)$ or v(CrO₃), 429 cm^{-1} v_2 (A_1) or v(Cr-Cl), 945 cm^{-1} $v_4(E)$ or v(CrO₃) cm^{-1}. UV/Visible and ^{1}H-NMR were all consistent with the TPPCC structure. Electronic at 451 nm, corresponding to 1a₂ 9e (= 173 M^{-1} cm^{-1}); 364 nm to 8e 9e (= 532 M^{-1} cm^{-1}); and 271 nm to 12a₁ 9e (=1279 M^{-1} cm^{-1}). UV/Visible, ^{13}C NMR and ^{1}H NMR were all consistent with the TPPCC structure.

Synthesis of Tetraphenylphosphonium Bromochromates (VI), $[(C_6H_5)_4P][CrO_3Br]$

Tetraphenylphosphonium Bromochromate can be easily prepared in excellent yield from the reaction of CrO_3 with Tetraphenylphosphonium Bromide in water in a molar ratio of 1:1. To a solution of chromium trioxide (1 g, 10 mmol) dry actonitrile (25 ml) was cooled to 0°C and a stoichiometric amoute of Tetraphenylphosphonium Bromide (4.19 g, 10 mmol) was added under stirring at room temperature. Within 1h, a clear orange solution fored which upon refrigerating gave solid TPPBC, which was isolated by filtration. The solid was washed with hexan and dried under vacuum for 1 h. $C_{24}H_{20}BrCrO_3P$: Cacld. %C, 55.49; %H, 3.85. Found: %C, 57.62; %H, 3.99. IR. (KBr): 905cm^{-1} $_1(A_1)$ or (Cro₃), 945 cm^{-1} $_4(E)$ or (Cro₃). UV/Visible was all consistent with the TPPBC structure. Electronic at 452 nm, Corresponding to 1a₂ 9e (= 174 M^{-1} cm^{-1}); 365 nm to 8e 9e (= 670 M^{-1} cm^{-1}); and 270 nm to 12a₁ 9e (= 1786 M^{-1} cm^{-1}).

Oxidation of alcohols: General Method

To TPPXC (0.001 mol) in CH_2Cl_2 (25 ml) was added the alcohol (0.001 mol) dissolved in a small amount of the solvent at room temperature. The mixture was stirred and refluxed for the time indicated in the Table 1 at room temperature, diluted with CH_2Cl_2 and filtered. Evaporation of solvent furnished the product. The molar ratio of substrate to oxidant was 1:1. The solution became homogeneous briefly before the black-brown reduced reagent precipitated. The progress of the reaction was monitored by TLC and UV/Vis spectrophotometry.

RESULTS AND DISCUSSION:

These reagents works as efficiently as activated manganese dioxide or Collins reagents. (15). These new oxidants efficiently oxidize number of organic substrates including primary, secondary alcohols. The results obtained with Tetraphenylphosphonium Halochromates are very satisfactory and show the new reagents to be a valuable addition to the existing oxidizing agents. (Table 1) summarizes the products, yields and reaction times of TPPXC with various substrates.
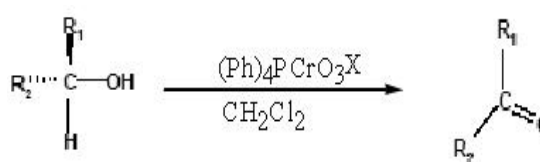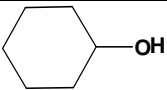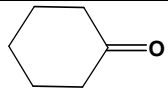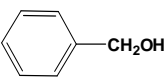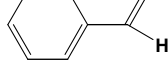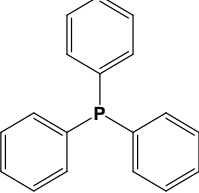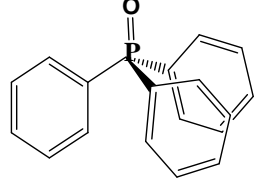
They concluded that the inequality between the Cr-O and the Cr-X bonds are responsible for the higher reactivity. TPPXC appears to be a stronger reagent than the others; these could be due to their lower symmetry. They have also been found that these reagents have certain advantages over similar oxidizing agents in terms of the amounts of oxidants and solvent required, and especially in the short reaction times required and in the higher yields of the product (Table I) (11,15,16).

Because of the stability and solubility of Tetraphenylphosphonium Halochromates, reactions could be performed at room temperature and the separation of the products is facile. During the reactions, the color of the oxidants changes from orange to brown, providing visual means for ascertaining the progress of

the oxidation. The mechanism for the presents oxidation are still unclear. However we assume that the mechanism of oxidation are similar to that of other Halochromates. In addition these oxidants and the oxidation conditions can be used for the synthesis of highly functionalized molecules.

Oxidations may also occur using only TPPXC, in the absence of wet SiO_2, but considerable improvements the yields and the corresponding reaction times are observed in the presence of the absorbent. These imply that the wet SiO_2 may act as a reaction medium, providing an effective heterogeneous surface area for the oxidation and at the same time making the work-up much more convenient.

Table1: Oxidations via TPPFC, TPPCC and TPPBC.

Sr. No.	Substrate	Product	TPPFC		TPPCC		TPPBC	
			Time (min)	Yield (%)	Time (min)	Yield (%)	Time (min)	Yield (%)
1	n-C_3H_7-OH	n-C_2H_5-CHO	170	92	160	90	150	90
2	2-C_3H_7-OH	2-C_2H_5-CHO	130	90	120	90	110	90
3	n-C_4H_9-OH	n-C_3H_7-CHO	120	94	110	93	110	91
4	2-C_4H_9-OH	n-C_3H_7-CHO	100	94	95	92	90	92
5	n-C_5H_{11}-OH	n-C_4H_9-CHO	90	90	85	88	80	87
6	n-C_8H_{17}-OH	n-C_7H_{15}-CHO	70	88	70	86	70	85
7			35	90	30	88	30	87
8			45	96	40	95	40	94
9			5	94	5	92	5	90

CONCLUSION:

The synthesized oxidants efficiently oxidize number of organic substrates including primary, secondary alcohols. TPPXC appears to be a stronger reagent than the others; these could be due to their lower symmetry. Oxidations may also occur using only TPPXC, in the absence of wet SiO_2, but considerable improvements the yields and the corresponding reaction times are detected in the presence of the absorbent. These suggest that the wet SiO_2 might act by way of a reaction medium, providing an effective heterogeneous surface area for the oxidation and at the same time making the work-up much more convenient.

REFERENCES:

1. Fieser LF, and Fieser M, **Wiley**, New York, Vols. 1967: 1-11.
2. Murugesan, V. and Pandurangan, A., Quinolinium Fluorochromate; A New Reagent for the Oxidation of Organic Compounds, **Indian Journal of Chemistry**, 31B: 1992: 377-378.
3. Mamaghani M., Shirini, F. and Parsa, F., Prolinium Chlorochromate as a New Mild and Efficient Oxidant for Alcohols, **Russ J Org Chem**, 38(8); 2002: 1113.
4. Shirini F., Mohammadpoor-Baltork I., Hejazi Z. and Heravi P. Caffeinilium Chlorochromate: As a Mild and Efficient Reagent for Oxidation of Alcohols and Chemoselective Oxidative Cleavage of Oximes, **Bulletin of the Korean Chemical Society**, 24(4): 517-518, (2003).
5. Srinivasan, R., Ramesh, C.V., Madhulatha, W. and Balasubramanian, K., "Oxidation of Alcohols by Quinolinium Chlorochromate" ***Indian J. Chem. Sec. B, 35B***, 480, (1996).
6. Guziec, F.S. and Luzzio, F.A., "The Oxidation of Alcohols Using 2,2 -Bipyridinium Chlorochromate", **Synthesis**, 1980: 691.
7. Tajbakhsh M., Hosseinzadeh R. and Yazdani-Niaki M. Synthesis and Application of 2,6- Dicarboxypyridinium Chlorochromate as A New Oxidizing Reagent for Alcohols, Silyl ethers and THP ethers under Mild and Non-aqeous Conditions, **J. Chem. Research (S),** 2002: 2.
8. Hosseinzadeh R., Tajbakhsh M. and Yazdani-Niaki M. 2,6-Dicarboxypyridinium Chlorochromate: a Mild, Efficient and Selective Reagent for Oxidative Deprotection of Oximes to Carbonyl Compounds, **Tetrahedron Lett.**, 43; 2002: 9413-9416.
9. Corey E.J., and Suggs, J.W. Pyridinium Chlorochromate; an Efficient Reagent for Oxidation of Primary and Secondary Alcohols to Carbonyl Compounds, **Tetrahedron Lett.**, 1975: 2647.
10. Corey E.J. and Schmidt G., Useful Procedures for the Oxidation of Alcohols Involving Pyridinium Dichromate in Aprotic Media, **Tetrahedron Lett**., 1979: 399-402.
11. Bhattacharjee M.N., Chaudhuri M.K., Dasgupta H.S. and Roy N., Pyridinium Fluorochromate; A New and Efficient Oxidant for Organic Substrates, **Synthesis**, 1982: 588-590.
12. Narayanan N. and Balasubramanian TR., Pyridinium Bromochromate-A New Reagent for Bromination and Oxidation, **Indian Journal of Chemistry**, 25B; 1986: 228-229.
13. Singh J., Kalsi P.S., Jawanda G.S. and Chhabra B.R., Quinolinium Chlorochromate; a Selective Oxidizing Agent, **Chemy Ind**., 1986: 751.
14. Kassaee M. K., Mahjob A. R. and Ghammami S., Tetramethylammonium fluorochromate(VI): a new and efficient oxidant for organic substrates", **Tetrahedron Letters**., 44; 2003: 4555-45557.
15. Collins J.C., Hess W.W. and Franck F.J., Dipyridine Chromium(VI) Oxide Oxidation of Alcohols in Dichloromethane, **Tetrahedron Lett.,** 9; 1968: 3363.
16. Srinivasan R., Stanley P. and Preethi, Balasubramanian K. Isoquinolinium Fluorochromate: A New and Efficient Oxidant for Organic Substrates, **Synth. Commun.,** 27; 1997: 2057-2064.
17. Ghammamy S, Mehrani K, Maleki S, Moghimi A, Shabaani F and Javanshir Z, Synthesis and Characterization of Two New Triphenylphosphonium Halochromates, $(C_6H_5)_3PH[CrO_3X]$, (X= F, Br) **Arkivoc**, 2007: 61-65.

RESEARCH ARTICLE

Synthesis and Characterization of Mikanecic acid Diesters using NaH

R.Nandhikumar[1,2]*, K. Subramani[1,3]
[1]R&D Centre, Bharathiar University, Coimbatore, Tamilnadu, India.
[2]Global Institute of Engineering and Technology, Tamilnadu, India.
[3]PG & Research Department of Chemistry, Islamiah College, Vaniyambadi, Tamilnadu, India.
*Corresponding Author E-mail: **nandhikumar@gmail.com**

ABSTRACT:
Catalysts are used to make changes easier in the organic synthetic mechanism. Catalysts are involved in the process of chemical changes by reducing time and making it faster to get things done. Catalysts play a vital role in organic synthesis with a novel method for the synthesis of a terpenoid, Mikanecic acid diester. In this research we are using NaH to synthesis Baylis-Hillman adducts (alkyl-3-hydroxy-2-methylenepropanoates reacts with aldehyde with a variety of acrylates catalyzed in presence of TiCl$_4$). Mikanecic acid diesters obtained from 1, 3-butadiene-2-carboxylate of (Diels-Alder type) self-dimerization occur in the presence of different catalysts. The yield which we obtained is in good ratio.

KEYWORDS: Baylis-Hillman adducts, Mikanecic acid diester, NaH, THF.

1. INTRODUCTION:

Synthetic organic chemistry is the paramount developing, expanding and successful branches of Science. During the past years, synthetic organic research has seen massive growth.[1-5] Development of new methods for the synthesis of heterocyclic compound, novel reagents, catalysts, strategies, and transformations is used. In synthetic organic chemistry, the constructions of quaternary carbon center have been one of the demanding and most attractive field due to a number of biologically active natural compounds consisting structural sub-units.[6-9] Terpenoid dicarboxylic acid and Mikanecic acid have attracted our attention due to its special feature of having vinylic quaternary carbon center. In 1936, Manske[10] isolated Mikanecic acid from the alkaloid Mikanoidine obtained by base hydrolysis of *Senecio mikakioides otto*. In literature[11] many research papers have been published based on the synthesis and characterization of Mikanecic acid.[12] Inorganic catalyzed organic reactions are obtaining importance owing to their low-cost nature and special catalytic attributes in various reactions.

In this view, our research is focused to develop environmentally benign protocols. Herein, we report, NaH [13-16] catalyzed synthesis of Mikanecic acid diesters results in fairly good yields.

In past years, many researchers developed the Baylis-Hillman reaction. In literature, DABCO [17] was used to perform this reaction and it resulted with the slow reaction rates. A Lewis acid (TiCl$_4$) reaction of acetaldehyde with appropriate acrylates successfully resulted with Baylis-Hillman adducts [18-19] (**1a-1c**). Then these adducts on treatment with suitable catalysts yielded with Mikanecic acid diesters (**2a-2c**) by Diels-Alder type (i.e. self-dimerization of 1, 3-butadiene-2-carboxylate) (Scheme **I Table 1**). Mikanecic acid diesters on hydrolysis gave Mikanecic acid. (**3**)

2. EXPERIMENTAL:

2.1 Materials and Methods

For this research, the use of chemical, reagents and solvent were bought from the real scientific company, India and used as such. Melting points were found out in an open capillary tube with a Buchi melting point apparatus. Elemental analyses were done by using Perkin-Elmer 240C CHN-analyzer. Perkin Elmer IR spectrophotometer records the ^{1}H- NMR spectra .This

was run in (CDCl$_3$) solvent at 200 MHz NMR spectrophotometer. In the same way ^{13}CNMR Spectra records the spectrum at 50 MHz.

2.2 Synthesis of Mikanecic Acid using NaH catalyst:

The synthetic procedure is very simple method. As shown in **Scheme I**. 0.01 Mole Baylis-Hillman adducts with THF in the presence of base catalyst (NaH) were refluxed for 2 hr. Then completion of their action monitored by TLC, common workup and column chromatographic purification (hex/ether, 5:1) gave products, which were characterized by IR, NMR spectral data. The outcomes obtained are very much consistent with literature report. The spectral and analytical data of the compound **2a-c.**

IR (neat): 1711, 1640 cm^{-1}; ^{1}H-NMR (200 MHz, CDCl$_3$): 1.71-1.92 (1H, m), 2.09-2.14 (1H, m), 2.22-2.44 (3H, m), 2.70-2.90 (1H, m), 3.71 (3H, s), 3.72 (3H,s), 5.10-5.22 (2H, m), 5.73-5.97 (1H, m), 6.91 (1H, m); Anal. Calcd for C$_{12}$H$_{16}$O$_4$: C, 64.21; H, 7.14 %.Found: C, 63.34; H, 6.90%.

Spectral data for Mikanecic acid: IR (KBr): 1691, 1641 cm^{-1}; ^{1}H-NMR (200 MHz, CDCl$_3$): 1.64-2.80(6H, m), 5.02-5.32 (1H, m), 5.72-6.04 (1H, m), 6.83(1H, m), 12.41 (2H, s, br); ^{13}C-NMR (50 MHz,CDCl$_3$): 21.53, 29.11, 31.74, 46.53, 114.53, 129.31, 136.73, 140.24, 167.60, 175.20; EI-MS: *m/z* 196 (M·); Anal. Calcd for C$_{10}$H$_{12}$O$_4$: C, 61.20; H, 6.11 %. Found: C, 57.43; H, 6.55 %.

Scheme: Synthesis of Mikanecic acid diester using NaH catalyst.

Scheme I

CH$_3$CHO + [Acrylate with COOR] →(TiCl$_4$, Chloroform)→ **1 a-c**

Acetaldehyde   Acrylate
R = Me,Et and t-Bu

Me,Et and t-Bu acrylate
Baylis -Hillman Adducts

NaH / THF   2 hr

Diels-Alder self Dimerization

2 a-c
Me, Et and t-Bu
Mikanecic acid diester

MeOH / KOH

3
Mikanecic acid
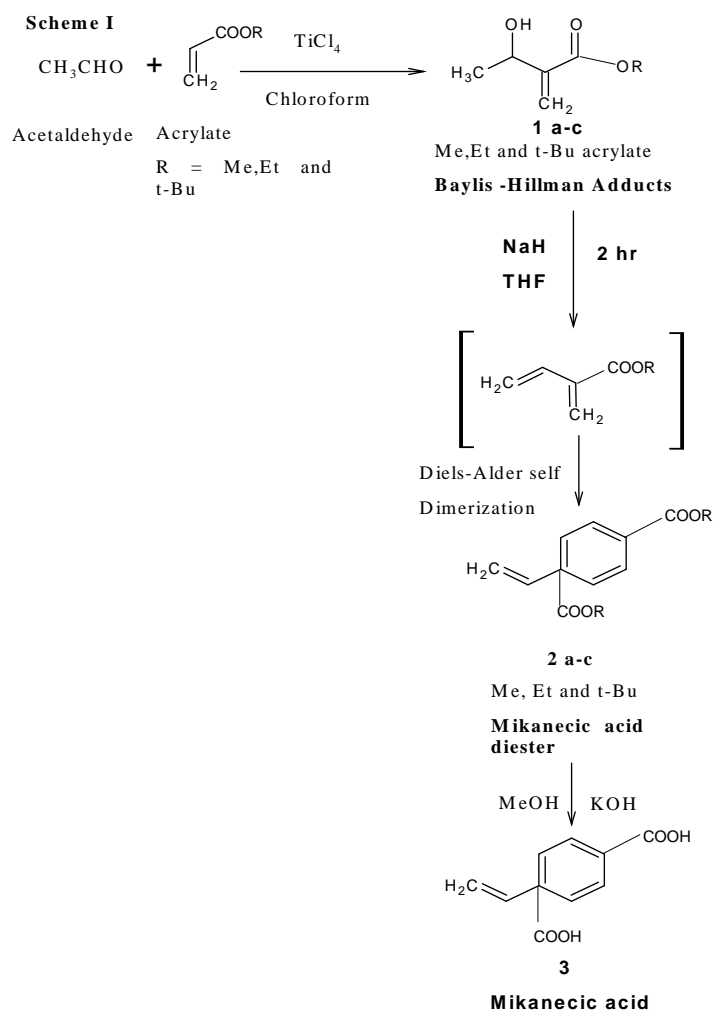
3. RESULT AND DISCUSSION:
3.1. Synthesis and Characterization:
The synthesis of Mikanecic acid diester from Baylis Hillman adducts using NaH catalyst. In this study first we prepared different Baylis Hillman adducts (**1 a-c**) by using acetaldehyde with different acrylates (Me, Et and t-Bu) in the presence of $TiCl_4$. Chloroform is used as solvent. Further these different Baylis Hillman adducts react with NaH Mikanecic acid diesters (**2a-c**) and which on hydrolysis gives Mikanecic acid (**3**). (**Scheme I**). All the synthesized compounds were characterized by IR, NMR and mass spectral analysis.

Table .1 Synthesis of Mikanecic acid diesters a, b and c (a-Me, b-Et and c-t-But acrylate).

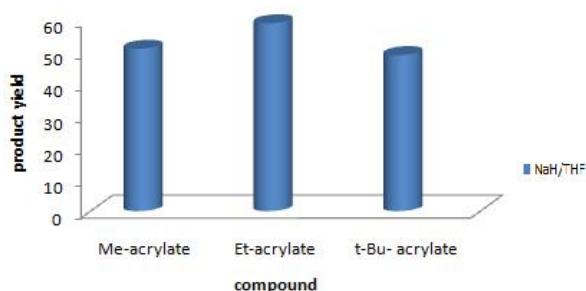| Substrate	Reaction time/catalyst	Product	Yield (%)
1a	2h /NaH	2a	51
1b	2h /NaH	2b	59
1c	2h /NaH	2c	49

Figure.1 Comparison of Different Acrylate with NaH for Synthesis of Mikanecic acid Diester.

4. CONCLUSIONS:
As a conclusion, this research describes a facile synthesis of Mikanecic acid diesters from Baylis-Hillman compounds, react with NaH and gives Mikanecic acid diesters, during Diels-Alder type self-dimerization of adducts (1, 3-Butadiene-2-carboxylate). The process represented was the indirect way of performing the Diels-Alder type method. In this method equal molecule of diene and dienophile react and resulted in Baylis-Hillman molecule.

5. ACKNOWLEDGMENT:
We whole heartedly thank the management, Principal of Global Institution of Engineering and Technology and Bharathiar University, R&D Centre for rendering full support for this work.

6. REFERENCES:
1. Salini.C.P et al. A Bibliometric evaluation of organic chemistry Research in India. Annals of library and information studies .61; 2014:332-342.URL: http://nopr.niscair.res.in/bitstream/123456789/30340/1/ALIS%2061%284%29%20332-342.pdf.
2. Francesco. Nicotra. Synthetic organic chemistry. Organic and biomolecular Chemistry. I URL: http://www.eolss.net/sample-chapters/c06/e6-101-03-00.pdf.
3. Dwivedi. S, Kumar. S and Garg. K .C. Scientometric profile of organic chemistry research in India during 2004-2013.Current science.109; 2015: 5-10.URL: http://www.currentscience.ac.in/Volumes/109/05/0869.pdf.
4. Nagaiah.K and Srimannarayana. G. Publications in organic chemistry from Indian universities and laboratories in 2011-2013 analysis and some suggestions. Current science. 108:2015:2-25.
5. Guoying Zhao et al. Mannich reaction using acidic ionic liquids as catalysts and solvents. Green Chem. 6; 2004:75-77.URL: http://www.iccom.cnr.it/aquachem/cvs/zhao.pdf.
6. Lushnikov.D.E and Babaev. V.Molecular Design of Heterocycles 4*. Utilization of computers in the chemistry of heterocycles(review).Chemistryof heterocyclic compounds. 29; 1993:10.URL: http://www.chem.msu.ru/eng/misc/babaev/papers/023e.pdf.
7. Akira Suzuki. Organoboranes in organic synthesis including Suzuki coupling reaction. Heterocycles. 80(1); 2010:15-43.URL: https://www.heterocycles.jp/newlibrary/downloads/PDF/21115/80/1.
8. Uladzimir ladziata and Viktor. Zhdankain. Hypervalent iodine (V) reagents in organic synthesis. ARKIVOC (IX); 2006:26-58.URL: http://www.arkat-usa.org/get-file/23541/.
9. Jianwei Han. Eco-catalysis leads the way to green synthetic chemistry. Han. organecic chem. Curr Res. 2012:1-1.URL: http://www.omicsonline.org/ecocatalysis-leads-the-way-to-green-synthetic-chemistry-2161-0401.1000e114.php?aid=8826
10. Manske. R.H.F, The alkaloids of *Senecio* species: II. Some Miscellaneous Observations. Canad. J. Res. 14B (1); 1936: 6-11.
11. Fuji. K, Asymmetric creation of quaternary carbon centers. Chem. Rev. 93(6); 1993: 2037.URL: http://pubs.acs.org/doi/abs/10.1021/cr00022a005.
12. Sydnes. L. K, Skattbol. L and Lappord. D.G Helv. Preparation of Mikanecic Ester and its precursor, 1, 3-butadiene-2-carboxylic ester Chim. Acta. 58; 1975:2061.URL: http://onlinelibrary.wiley.com/doi/10.1002/hlca.19750580721/abstract.
13. Sun Qi and Sun Ren-an. Hydrogenation of Olef ins Catalyzed by Highly Active Titanocene/ NaH or n-BuLi Catalyst Systems. Chem. Res. Chinese U.18 (3); 2002:307-310.URL:http://www.cjcu.jlu.edu.cn/hxyj/EN/abstract/abstract13814.shtml
14. Yin-Heng Fan et al. Extremely Active Catalysts for the Hydrogenation of Terminal Alkenes. Journal of catalysis. 205; 2002:294-298.URL: http://www.sciencedirect.com/science/article/pii/S0021951701934293.
15. Hery Suwito et al. Chalcones: Synthesis, structure diversity and pharmacological aspects. Journal of chemical and pharmaceutical research, 6(5); 2014:1076-1088.URL: *https://www.researchgate.net/file.PostFileLoader.*
16. Takashi Ooi and Keiji Maruoka. Recent Advances in Asymmetric Phase-Transfer Catalysis. Angew. Chem. INt.E. 46; 2007:4222-4266.URL: http://onlinelibrary.wiley.com/doi/10.1002/anie.200601737/abstract.
17. Deevi Basavaiah, Anumolu Jaganmohan Rao and Tummanapalli Satyanarayana. Recent Advances in the Baylis-Hillman Reaction and Applications. Chem. Rev, 103; 2003: 811-891.URL: http://isites.harvard.edu/fs/docs/icb.topic208898.files/Week_of_Nov_26th/basavaiah_baylis_hillman_review.pdf.
18. Jeong Beom Park et al. Synthesis of Indanones via Intramolecular Heck Reaction of Baylis-Hillman Adducts of 2-Iodobenzaldehyde. Bull. Korean Chem. Soc.25 (6); 2004:927.URL: *www.journal.kcsnet.or.kr/.../j.../j_download.htm.*
19. Alan R. Katritzky et al. The Baylis-Hillman reaction of substituted Aminomethylbenzotriazoles. ARKIVOC. 3; 2008: 91-101.URL: http://www.arkat-usa.org/get-file/23109/.

www.ajrconline.org

ajrc

RESEARCH ARTICLE

Synthesis of 2-acetylfuran by vapor phase acylation of furan over ferrite

Naseeb Singh*, R. K. Gupta
Department of Chemistry, Guru Jambheshwar University of Science and Technology, Hisar (Haryana) 125001, India.
*Corresponding Author E-mail: **nsdchem@gmail.com**

ABSTRACT:
The synthesis of 2-actylfuran using from furan using acetic anhydride as an acylating agent via vapor phase catalysis has been reported. The influence of molar ratio, temperature and weight hour space velocity (WHSV) on yield of 2-actylfuran are investigated. The yield and selectivity of 2-actylfuran were observed to be 89.07% and 99.71%, respectively at temperature 573 K, WHSV 0.3 h^{-1} and molar ratio 1:4 on Co^{2+} /Ni^{2+}/Cr^{+2} ionic distribution in the spinel lattice effects the acidic-basic properties. It was also observed that catalytic activity of ferrites was influenced by the acidity of catalyst.

KEYWORDS: Vapor phase acylation, ferrites, selectivity, 2-acetylfuran, acetic anhydride, furan.

1. INTRODUCTION:

Transition metal ferrites have attracted great attention because of their significant magnetic, electrical and catalytic properties [1-2]. The use of ferrite as heterogeneous catalysts over homogenous catalyst has led to enhanced reaction rates, better selectivity, high yield and simple workup[3-5] These catalyst are possessing remarkable magnetic properties and can be easily recovered from the reaction mixture. A variety of metal ferrite such as copper, nickel, chromium, cobalt, zinc and mixed metal ferrite have been developed and utilized in varias organic transformation for catalytic purposes [6-7]. The crystalline structure of metal ferrite $M^{2+}_{tet}.[Fe^{3+}_{octa}]O_4$ is spinel, where M is Co, Ni, Cr. The distributions of metal ion between tetrahedral and octahedral are influence by acido-basic properties of ferrospinels [8-9].

Furan and its derivatives are important heterocyclic compounds used as intermediates in drugs, pharmaceutical industries, research laboratories, etc. [10-11]. 2-actylfuran is an important intermediate to HIV-integrase S-1360 inhibitor [12]. Friedal-Craft acylation of furan using homogeneous catalytic system like $AlCl_3$, $FeCl_3$, $TiCl_3$, is the conventional and classical method for the synthesis of 2-actylfuran . Holdrich *et al.* reported the synthesis of 2-acetylfuran with 99% selectivity and 23% conversion of furan over Ce-doped boron zeolite [13]. Reddy *et al.* reported the acylation of furan with acetic anhydride over zeolites as heterogeneous catalytic system with 67.5% conversion of furan [14]. In view of the above and in confirmation of our continuing investigation of ferrite ferrospinels as catalytic system, herein we report the vapor phase synthesis of 2-actylfuran from furan and acetic anhydride using ferrites with improved yield reported compared to the literature.

2. EXPERIMENTAL:

2.1. Preparation of CoFe$_2$O$_4$ (NSF1)
Ferrites are prepared by using co-preparation method reported in the literature [15-17].

2.2. Preparation of other catalysts
The other catalysts were also prepared by following the same method as for $CoFe_2O_4$ (NSF1), there are variation

in number of moles of metal. $Ni_{0.5} Co_{0.5}Fe_2O_4$ (NSF2) was prepared by taking 0.0375 mol of $NiCl_2$ and 0.0375 mol of $CoCl_2$, at the place of 0.075 mole of $CoCl_2$, and $Co_{0.5}Cr_{0.5}Fe_2O_4$ (NSF3) was prepared by taking 0.0375 mol of $CoCl_2$ and 0.0375 mol of $CrCl_2$. Likewise, $Ni_{0.5}Cr_{0.5}Fe_2O_4$ (NSF4) was prepared by taking 0.0375 mol of $NiCl_2$ and 0.0375 mol of $CrCl_2$ and $Ni_{0.33} Co_{0.33} Cr_{0.33}Fe_2O_4$ (NSF5) was prepared by taking 0.025 mol of $NiCl_2$, 0.025 mol of $CrCl_2$ and 0.025 mol of $CoCl_2$. [15-17]

2.3. Catalyst characterization, surface area and acidity measurements

Catalysts were characterized by FTIR, X-ray diffraction (XRD), BET surface Area and ammonia-TPD methods. FTIR spectra were recorded on Shimazdu 8000 spectrophotometer. Two major bands were observed around 700 cm^{-1} and 500 cm^{-1}. These bands indicate that formation of spinel structure having tetrahedral and octahedral arrangement of ion. Absorption band around 700 cm^{-1} is attributed to the tetrahedral sites, and band observed around 500 cm^{-1} is indicates octahedral sites which are in agreement with reported data in the literature [18]. X-ray diffraction of NSF1, NSF2, NSF3, NSF4 and NSF5 was recorded on a Rigaku diffractometer with Cu-Ka radiation and is reproduced. The observed X-ray peaks matches with the characteristic reflections of corresponding ferrites and confirm the phase purity of samples.

To determine the acidity values of all the ferrite catalysts temperature programmed ammonia desorption (NH_3-TPD) method was used. 1.0 g of the sample was taken in the tube and heated up to 673 K with under nitrogen atmosphere for 2 h followed by cooling down to 298 K. Then the sample was exposed to ammonia for 2 h and sample was flushed with nitrogen for 1 h to desorb the loosely bound ammonia molecules on the sample. The sample was again heated to 423 K, so that physically adsorbed ammonia get desorbed which corresponds to weak acidic sites. The temperature of the sample was then raised to 623 K and the amount of desorbed ammonia was estimated. The ammonia desorbed in this temperature range was considered to represent medium acidic sites. Further, this desorption process was repeated at 723 K; the ammonia desorbed in this region was considered to represent strong acidic sites. Quantitative estimation was made by volumetric analysis and results are presented in Table1. The BET surface areas of ferrites were determined on Quantachrome Autosorb Automated Gas Sorption System Report Autosorb 1 for Windows 1.55 .instrument; the results are depicted in Table-1.

2.4 Apparatus and procedure

On fixed-bed micro reactor having 0.45 m length and 13 mm diameter was used to determined catalytic activities. The lower half worked as reactor and upper half worked as preheater. The ferrite was packed between two plugs of glass wool. The catalyst was activated at 773 K with the flow of air for one hour. Then start the flow of nitrogen gas to down the desired temperature about 373K. Now set the flow of nitrogen gas of 30 mL/min and reactants were fed from the top. In condenser the cold water was used to condense gaseous products. To analyze the liquid product mixture we have to use gas chromatograph FID, SE-30 column. The activity of ferrites data comparison is made between different catalysts at 2h duration run. There was negligible thermal conversion when a blank run was taken without any catalyst.

Table 1

Catalysts	423-523K	523-623K	623-723K	Total acidity mmol/g	BET Surface area (m^2/g)
NSF1	0.42	0.40	0.39	1.21	58.11
NSF2	0.43	0.41	0.40	1.24	57.80
NSF3	0.44	0.43	0.40	1.27	48.85
NSF4	0.46	0.42	0.41	1.29	46.36
NSF5	0.47	0.44	0.42	1.33	39.91

BET surface areas (m^2/g) and catalytic acidity at different temperatures. [19]

3. EFFECT OF REACTION PARAMETER.
3.1. Variation of catalyst

Effect of variation of catalyst was tested for the selection of most appropriate catalytic system and the results are depicted in table 2.

Table 2

Catalyst	% Conversion	% Yield	Selectivity
NSF1	84.76	69.12	98.01
NSF2	91.80	83.32	99.03
NSF3	86.34	72.67	98.90
NSF4	87.40	75.43	99.10
NSF5	94.12	89.07	99.71

From the data of table 2, all the tested ferrites are found to be active catalysts for furan acylation with acetic anhydride under observed conditions. The catalytic activity of different catalysts were found to be in order NSF5>NSF2>NSF4>NSF3> NSF1. The maximum yields of acylated products obtained was 89.07 % of 2-actyle furan with selectivity 99.71 % on NSF-5 catalyst .The other products formed in negligible amounts on optimized condition (molar ratio 1:4, WHSV 0.3 h^{-1} and temperature 573 K). The $Ni^{2+}/Co^{2+}/Cr^{+2}$ ionic distribution in the spinel lattice of catalyst NSF-5 plays important role for high yield and selectivity.

Table 3

Effect of temperature on acylation of furan (catalyst NSF5, WHSV 0.3 h^{-1} and molar ratio 1:4)

Temperature (K)	% Conversion	% Yield	Selectivity
473	34.97	27.14	86.18
523	92.62	76.81	97.93
573	94.12	89.07	99.71
623	91.42	80.54	98.46
673	75.11	62.31	98.01

3.2 Effect of temperature.

An effect of temperature on acylation of furan acetic anhydride was studied over (NSF-5) in the temperature range 473-673 K, WHSV 0.3 h^{-1} and molar ratio 1:4; the results are shown in table 3. Therefore the investigation of acylation of furan was restricted to only 573 K, where the yield of 2-actylfuran is high in comparison to the values reported in literature in each acylation reaction. It was also found that the decrease in the yield of the acylated product at higher temperatures is due to the charring of some reactants. These observations draw our attention to conclude that the strong and medium acidic sites favor vapor phase acylation of furan. The activity of catalyst goes decrease with increase the temperature.
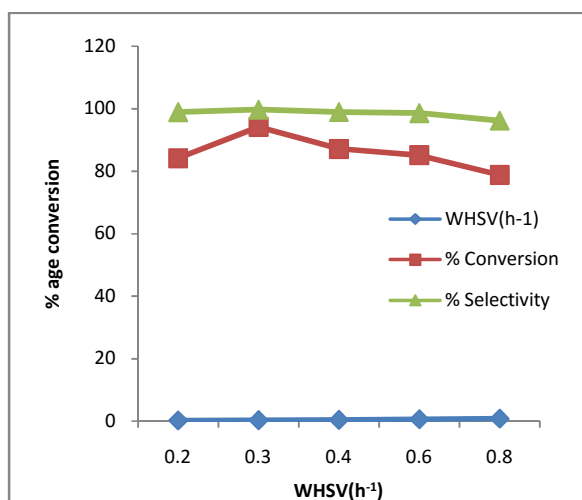

Fig. 1: Effect of WHSV on acylation of furan (catalyst NSF5, temperature 573 K and molar ratio is 1:4)

3.3. Variation of WHSV.

The effect of WHSV on acylation of furan was studied over (NSF-5) catalyst at a temperature of 573K, at 1:4 molar ratio of furan : acetic anhydride and WHSV (0.2, 0.3, 0.4, 0.6 and 0.8 h^{-1}). The results are shown in fig.2. Furan conversion increased as the WHSV increased from 0.2 to 0.3 h^{-1} and decreased thereafter. The more contact time of catalysts and feed causes charring over active sites, hence decreasing the furan conversion. Below 0.3 h^{-1} WHSV furan conversion was decreased due to the low contact time of feed and the catalyst. Hence the best yield of acylated products on 0.3 h^{-1}, that is optimum weight hour space velocity.
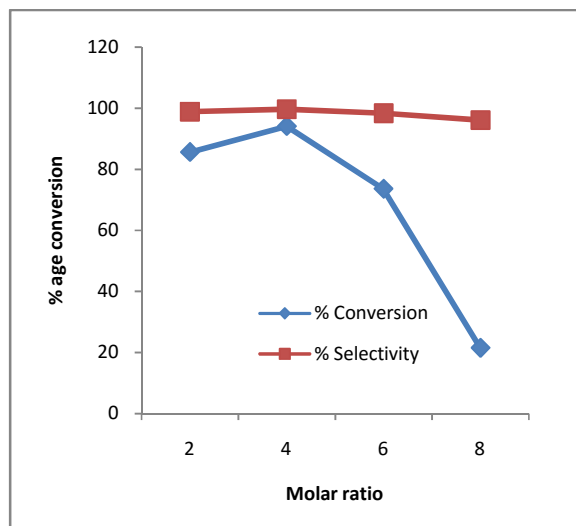

Fig. 2: Effect of molar ratio on acylation of furan (catalyst NSF5, temperature 573 K and 0.3 h^{-1}WHSV)

3.4. Variation of molar ratio.

As seen from the results in fig.2., the molar ratio of furan : acetic anhydride varied from 1:2 to 1:8 and the vapor phase acylation of furan was carried out over NSF-5 at temperature 573 K and WHSV 0.3 h^{-1}. Furan conversion and selectivity of 2-actyle-furan increased with increase in the furan-to-acetic anhydride molar ratio, reaching a maximum at 1:4. At higher molar ratio, the selectivity and conversion of 2-actylefuran was reduced. This was probably due to the unavailability of active sites for furan over the catalyst surface, because of competition between furan and acetic anhydride adsorption
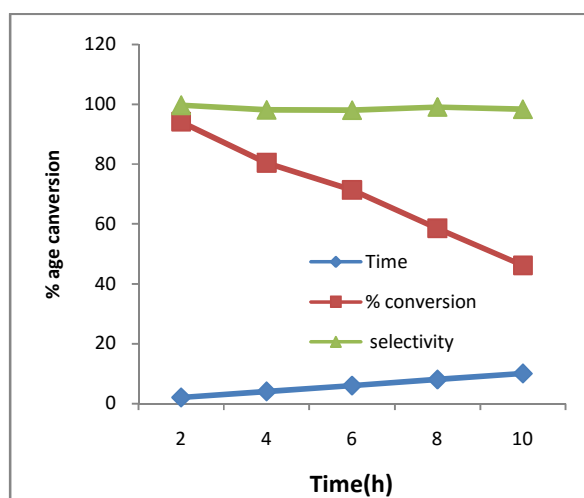

Fig. 3: Effect of time on stream (TOS)

3.5. Effect of time on stream (TOS)

The acylation of furan was carried out for 10 h on all the ferrites. Under optimized conditions the highest conversion was obtained on catalyst NSF-5 at temperature 573 K, WHSV 0.3 h^{-1} and molar ratio 1:4. It has been observed that there was continuing decrease of catalytic activity with increasing time. The results are shown in fig. 3. The acylated products decreased gradually with time on stream, but selectivity is not very much affected. This may be due to coke formation on the surface of catalysts or due to deactivation of ferrite.

4. MECHANISM:

The aromatic five-membered heterocyclic compounds all undergo electrophilic substitution. Electrophilic substitution at 2- or 3-position is readily likely to occur. Further, quantitative results derived by molecular orbital method applied to furan show greater p-electron density at 2-position than at 3-position. Dewar gave a qualitative explanation to this difference in reactivity [20-22].
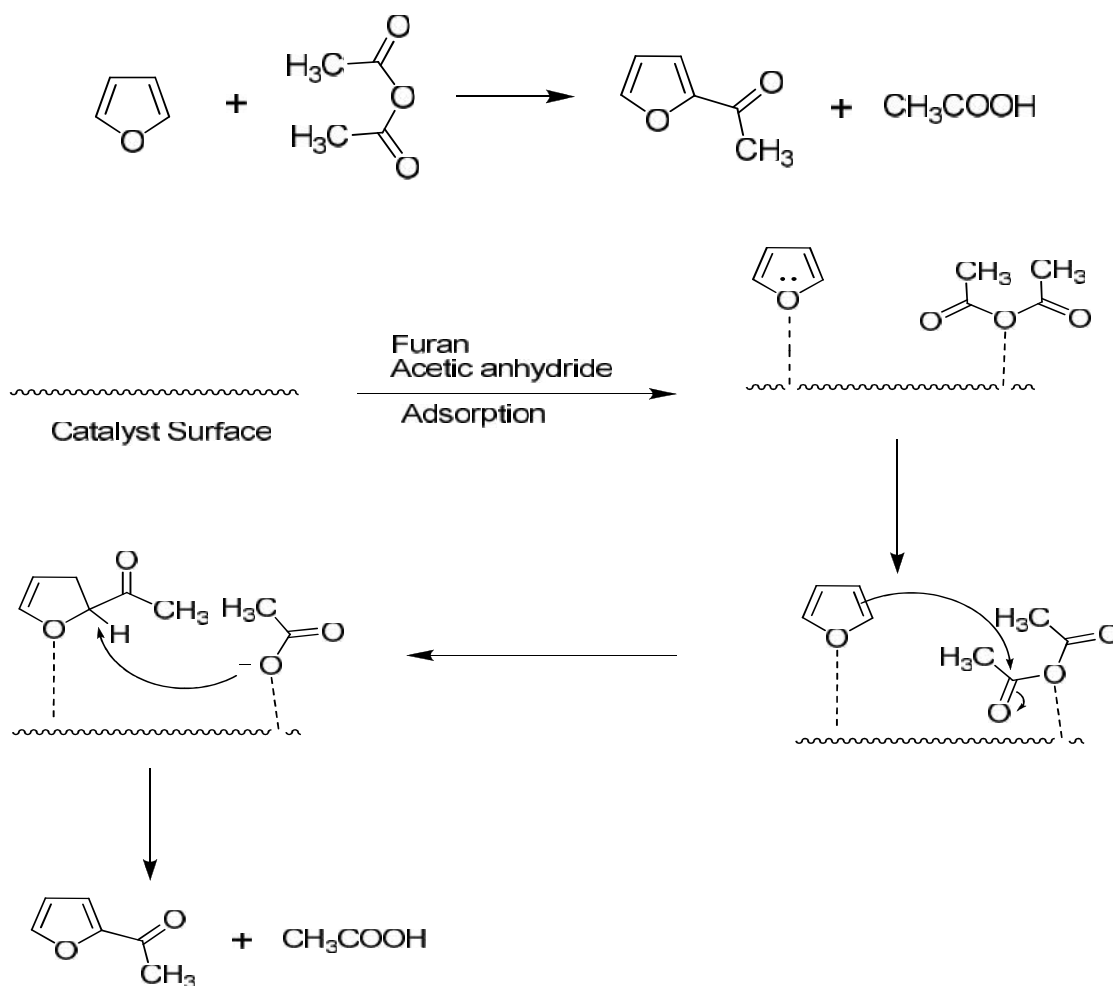
5. CONCLUSIONS:

In conclusion, catalysts NSF1, NSF2, NSF3, NSF4 and NSF5 prepared via low temperature co-precipitation method are utilized for acylation of furan with high yields of 2-aceylfuran compared to the literature. The catalytic activity experiment reveals that strong and medium acidic sites are suitable for the acylation of furan. The catalytic activity of the system was dependent on the reaction parameters and maximum yield of 2-acetylfuran was achieved on NSF-5 catalytic system. The maximum yield of acylated product obtained was 89.07 % of 2-actylefuran with 99.71% selectivity, with negligible side products over NSF-5 ferrite and acylating agent is acetic anhydride, at molar ratio 1:4, WHSV 0.3 h^{-1} and temperature 573 K.

6. REFERENCES:

1. Lu H C, Juu E C, Weng W V, Hung T C and Ying Li C. **International Journal of the Physical Sciences**. 6 (4); 2011: 855-865.
2. Siwach P, Singh S and Gupta R K. **Catalysis Communications**. 10; 2009: 1577-1581.
3. Rajendra S, Gaikwad, Sang Y C, Rajaram S, Mane, Sung H and Oh S J. **International Journal of Electrochemistry**. 2011; 2011: 1- 6.
4. Wei C H, Chen S C, Kuo P C, Lie C T and Tsai W S. **Material Science and Engineering B**. 111; 2004: 142-149.
5. Sethuraman G, Oriparambil S, Nirmal G, Sathishkumar S, Sudhakara P, Jayaramudu J, Ray S S and Annamraju K V. **Applied Science Letters**. 1(1); 2015: 8-13.
6. Reddy V S, Shyam A R, Dwivedi R, Gupta R K , Chumbale V R and Parsad R. **Journal of Chemical Technology and Biotechnology**. 79; 2004: 1057-1064.
7. David G, Raquel SG, Joseph G, Yurii K and Gun K. **Nanomaterials**. 4; 2014: 331-343.
8. Junfeng W, Wenhong P, Changzhu Y, Man Z, Jingdong Z. **Journal of Environmental Sciences**. 25(4); 2013: 801-807.
9. Siwach P, Singh S and Gupta R K. **International Journal of Chemical Sciences**. 6 (2); 2008: 1041-1049.
10. Jin P C, Yun L, Xiao Q Z, Yongkai S, Feng B, and Jiaqi H. **Journal of Organic Chemistry**. 65; 2000**:** 3853-3857.
11. Fujsawa T, Kondo K and. Sakai K. **US Patent**, **US**. 4266067. 1981.
12. Kenji I, Mikio K, Masaaki U and Sumio S. **Organic Process Research & Development**. 11; 2007: 1059-1061.
13. Holderich, W F. **Studies in Surface Science and Catalysis**. 49; 1989: 69.
14. Reddy P R, Subrahmanyam M and Kulkarni S J. **Catalysis Letters**. 54; 1998: 95-100.
15. Sreekumar K, Mathew T, Rajgopal R, Vetrivel R and Rao B S. **Catalysis Letters**. 65; 2000: 99-105.
16. Rao B S, Sreekumar K and Jyothi T M. **Indian Patent**. 2707; 1998: 98.
17. Sreekumar K, Mathew T, Devassy B M, Rajgopal R, Vetrivel R and Rao B S. **Applied Catalysis A: General**. 205; 200: 11-18.
18. Pawan S, Surander S and Gupta R K. **Applied Catalysis A: General**. 366; 2009: 65–70.
19. Naseeb S and Gupta R K. **Asian Journal of Research in Chemistry**. 9 (2); 2016:
20. Bansal R K. **Heterocyclic Chemistry (Syntheses, Reactions and Mechanisms**) Wiley Eastern Ltd., New Delhi (India).1990: 105-123.
21. Joule J A, Smith G F. **Heterocyclic Chemistry**, 2nd, ELBS and VNRC Ltd. London.1978: 192-219.
22. Dewar M J S. **Electronic Theory of Organic Chemistry**, **Oxford**. 1949: 188.

ajrc

RESEARCH ARTICLE

Determination of major tobacco alkaloids in mainstream cigarette smoking

C. C. Kurgat[1], J. K. Kibet*[1], P. K. Cheplogoi[1], S. C. Limo[2], and P. M. Kimani[1]
[1]Department of Chemistry, Egerton University P.O Box 536 - 20115, Egerton, Kenya
[2]Department of Physics, University of Eldoret, P.O. Box 1125-30100, Eldoret, Kenya
*Corresponding Author E-mail: **jkibet@egerton.ac.ke**

ABSTRACT:
The popularity of tobacco use worldwide has kicked off one of the greatest clinical debates on human toxicology and public health in general. Accordingly, this study investigates some of the alkaloids in tobacco believed not only to be addictive and carcinogenic but also as precursors for other related medical problems. The characteristic behaviour, identification and product evolution of -nicotyrine and 3,5-dimethyl-1-phenylpyrazole in tobacco is reported extensively in this study for the first time. Two commercial cigarette brands coded SM1 and ES1 were explored for evolution of major alkaloids over a modest temperature range of 200 – 700 °C for a total pyrolysis time of 3 minutes using a tubular quartz reactor, typically in increments of 100 °C using nitrogen as the pyrolysis gas at a residence time of 2.0 seconds under 1 atmosphere pressure. The heating rate of the heater was ~ 20 °C s^{-1}. The pyrolysate was passed over 10 mL analytical grade methanol and analyzed using a Gas-Chromatography hyphenated to a mass spectrometer (GC-MS) with a mass selective detector (MSD). GC-MS results showed that nicotine was the major alkaloid in both cigarettes reaching a maximum at ~ 400 °C (8.0 x 10^8 GC-Area counts) for ES1 cigarette and 500 °C (~2.7 x 10^8 GC-Area counts for SM1 cigarette. Clearly, the ratio of nicotine for ES1 to SM1 is approximately 3 indicating that ES1 cigarette is rich in nicotine. Based on this data alone, ES1 cigarette was found to be more addictive.

KEYWORDS: Alkaloid, pyrolysate, toxicology, -nicotyrine.

INTRODUCTION:
Smoking has serious effects on almost every organ in the body, accounting for more than 10% of deaths from all causes and 30% of deaths from cancer related cases worldwide[1,2]. According to the Global Burden of Disease study, smoking causes incredible ill health, estimated at 2,276 disability-adjusted life years (DALYs) per 100,000 tobacco consumers[3]. Accordingly, whereas studies on nicotine is widely reported literature, research on -nicotyrine and 3,5-dimethyl-1-phenylpyrazole alkaloids is yet to gain significant attention. Therefore, this study is one of the first to explore the evolution of -nicotyrine and 3,5-dimethyl-1-phenylpyrazole in a more detailed approach. The alkaloid family in tobacco is known to be responsible for addiction in cigarette smoking therefore their investigation is very important[2,4]. Generally, Cigarette smoking is believed to be responsible for serious health, and public health problems throughout the world [5]. In addition, cessation of cigarette smoking is particularly difficult because of the highly addictive nature of nicotine [6]. Among regular smokers, withdrawal symptoms occur within two hours of the last cigarette, peaking within 24–48 hours and sometimes may last for weeks or in some cases even months[3]. These revelations are disturbing considering that tobacco is the leading cause of preventable death in the world [7-9].

The symptoms of cigarette withdrawal are psychological and include the desire to smoke, depression, sleeplessness, irritability, anxiety, difficulty concentrating, restlessness, and weight gain [10]. Most

smokers who quit smoking experience nicotine withdrawal symptoms due to nicotine dependence [11]. Usually the symptoms are most severe during the first 3 days after cessation but may continue for weeks or even months [12]. The severity of these symptoms depends on the number of cigarettes smoked daily and the duration of usage [2,4,13]. Research has also proven that women are unfortunately less successful in quitting smoking than men[4,14] because the withdrawal symptoms of nicotine and possibly other alkaloids are more severe in women and replacement therapy has proven to be less effective [15].

The molecular structures of alkaloids explored in this study are presented in Fig. 1. Nonetheless, other minor alkaloids such as 3-methyl pyridine, and 2-methyl pyrrole, have briefly been discussed in this work from the mechanistic destruction of nicotine in high temperature smoking regime.
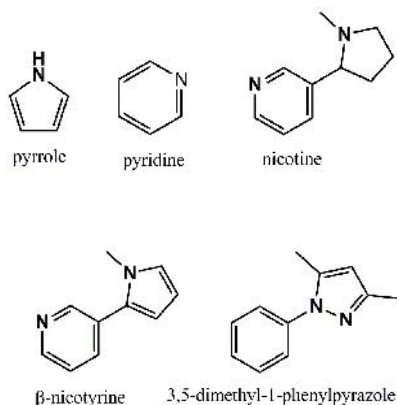

Fig. 1: The molecular structures of alkaloids investigated in this work

Considering the complex nature of tobacco smoke, with more than 7,000 known constituents, and its biological variety characterized by the presence of carcinogens, toxicants, irritants, tumor promoters, co-carcinogens, and inflammatory agents, any determination to identify individual compounds which cause lung cancer, oxidative stress or cardiac arrest in smokers is difficult[16,17]. Therefore, the concept of tobacco development, composition, and toxicity is no doubt a very important area of research [18]. Inhalation studies of cigarette smoke have many difficulties which have been previously summarized, all relating to the fact that laboratory animals do not voluntarily inhale cigarette smoke, but rather try to avoid it [17,19]. Nevertheless, a number of relatively recent studies have demonstrated lung tumor induction in both rats and mice exposed to cigarette smoke [16,19].

This study focuses primarily on the evolution of major tobacco alkaloids at various smoking temperatures using an in-line GC-MS at specific temperature at which they are evolved in high amounts during cigarette smoking. The temperature at which the concentration of alkaloids are released in high amounts is important especially in designing modern cigarettes that can be smoked at lower temperatures thus avoiding consumption of high levels of alkaloids by smokers. Mechanistic description for the formation of free radicals from nicotine considered biologically harmful has been explored quantum mechanically. Furthermore, interesting conclusions have been drawn regarding the evolution of nicotine from the two common cigarettes (ES1 and SM1). A toxicological survey of these alkaloids based on our data and literature data has been briefly discussed.

EXPERIMENTAL PROTOCOL:
Materials
The heater (muffle furnace) was purchased from Thermo Scientific Inc., USA while the quartz reactor was locally fabricated in our laboratory by a glass-blower. Commercial cigarettes SM1 and ES1 (for confidentiality) were purchased from retail outlets and used without further treatment. Methanol (purity 99%) used to dissolve cigarette pyrolysate was purchased from Sigma Aldrich Inc. (USA).

Sample preparation
50 mg of tobacco was accurately weight to the nearest mg and packed in a quartz reactor of dimensions: i.d. 1 cm x 2 cm (volume $\approx$ 1.6 cm^3). The tobacco sample in the quartz reactor was placed in an electrical heater whose maximum heating temperature is 1000 ˚C with a heating rate of ~ 20 ˚C s^{-1}. The tobacco sample was heated in flowing nitrogen pyrolysis gas to maintain a residence time of 2.0 s and the smoke effluent was allowed to pass through a silica coated transfer column and collected in 10 mL methanol in a conical flask for a total pyrolysis time of 3 minutes and sampled into a 2 mL crimp top amber vials for GC-MS analysis. This combustion experiment was conducted under conventional pyrolysis described elsewhere [20] and the evolution of alkaloids (nicotine, -nicotyrine, 3,5-dimethyl-1-phenylpyrazole, pyrrole, and pyridine) were monitored between 200 and 700 ˚C.

GC-MS identification of tobacco alkaloids

GC-MS analysis was carried out using an Agilent Technologies 7890A GC system coupled with an Agilent Technologies 5975C inert XL Electron Ionization/ Chemical Ionization (EI/CI) with a triple axis mass selective detector (MSD), using HP-5MS 5% phenyl methyl siloxane column (30 m x 250 µm x 0.25 µm). The temperature of the injection port was set at set at 200 ˚C to vapourize organic components to the gas-phase prior to MS analysis. The carrier gas was ultra-high pure (UHP) helium (99.99%). The flow rate of the carrier gas (He) was set at 3.3 mL/min at 1 atmosphere pressure and a residence time of 2.0 seconds. Temperature programming was applied at a heating rate of 15˚C for 10 minutes, holding for 1 minute at 200˚ C, followed by a heating rate of 25 ˚C for 4 minutes, and holding for 10 minutes at 300 ˚C. Electron Impact ionization energy of 70 eV was used. To ensure that the right alkaloid was detected, standards were run through the GC-MS analytical system and the peak shapes and retention times compared with the compounds of interest.The data was run through the NIST library database as an additional tool to confirm the identity of compounds[20].

GC-MS analysis Quality Control (QC)

To ensure consistency in GC-MS data the mass spectrometer was tuned to check for leaks and water levels in the instrument which would affect the accuracy of the data before any analysis was conducted. This procedure was very important in order to prevent contamination, and extend the life of the EI filament. Quantitative transport tests were initiated before any run was conducted to ensure that there were no leaks in the GC-MS system and guarantee the pyrolysis system is clean. The flow rate in the transfer line was monitored to make sure that it was constant and did not fluctuate. If the flow rate was not consistent, and the pressure was not stable when the transfer line was connected to the GC-MS then leaks could be present in the system. This was corrected before any experiment could begin. To correct for any leaks in the system, a gas leak detector was used. Whenever leaks were detected along the gas lines, transfer lines, or reactor-injection port interface, the connections were tightened and quantitative transport experiment repeated to make sure no leaks were in the system. A known concentration of nicotine was injected into GC-MS system to monitor how much nicotine was recovered after analysis. This was to test the efficiency of the GC-MS instrument. A recovery of 95% was good enough in order to proceed with analysis.

Computational methodology

In order to investigate the molecular behaviour and energetics for formation of free radicals from nicotine, thermochemical calculations were conducted using Gaussian '09 computational framework. Nicotine was used as the test compound for selecting a suitable basis set (cf. scheme 1 and Figure 2). The geometries were optimized at DFT/B3LYP using the 6-31G basis set [21]. When using DFT, however; the choice of basis set is considered to be inconsequential because the convergence of DFT to the basis-set limit with increasing size of basis set is relatively fast and thus small basis sets are used[21, 22]. More often, diffuse functions on basis sets are not used for DFT calculations, as these lead to linear dependencies and a bad convergence of the self-consistent-field (SCF) Kohn–Sham equations for larger molecules [22].

RESULTS AND DISCUSSION:

In this study, it was established that the alkaloid content varied widely among the two commercial cigarettes investigated as shown in Fig, 2. Nonetheless, one thing was remarkable that most combustion alkaloids were released in high quantities between 400 – 500 ˚C contrary to previous biomass pyrolysis experiments which put the evolution of most by-products at between 300 and 400 ˚C [20,23]. Pyro-synthesis of alkaloids during tobacco burning is therefore unique probably because of the high energies involved during the formation of the C-N bonds. As a result, the product evolution of major alkaloids is shifted to higher temperatures. However, pyrrole for instance has a maximum release at ~ 450 ˚C which is consistent with previous pyrolysis experiments on biomass pyrolysis [24]. It is important to note that whereas studies on product evolution agree on a given temperature range of maximum release of reaction products, the pyrolysis conditions and type of biomass under study may cause the pyrolysis products to be released either at lower or higher temperature ranges. Nevertheless, consensus of opinion agrees that most combustion by-products reach a maximum between 400 and 500 ˚C [25].
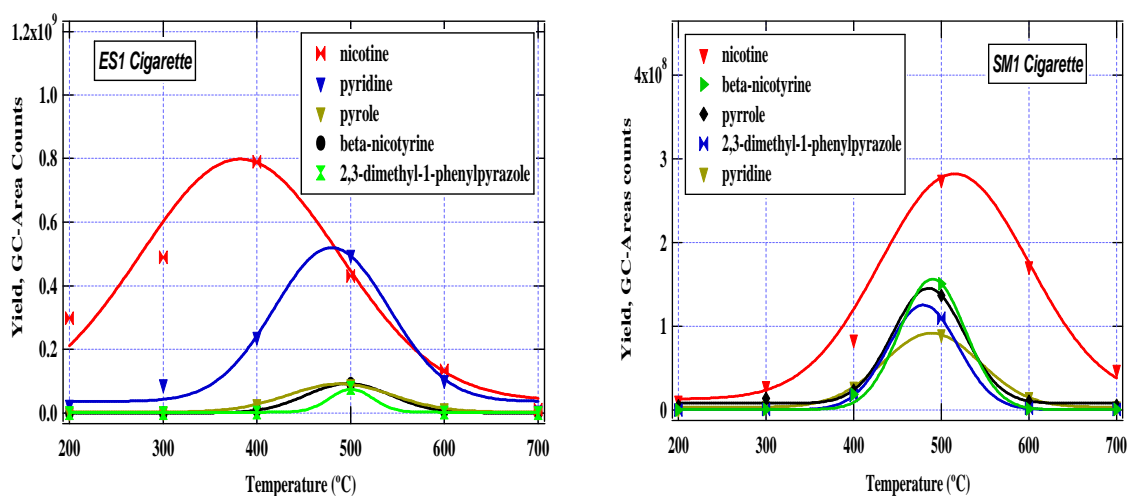
Fig. 2: Product distribution of nicotine and major alkaloids in mainstream cigarette smoke determined from the burning of two commercial cigarettes; ES1 (left) and SM1 (right).
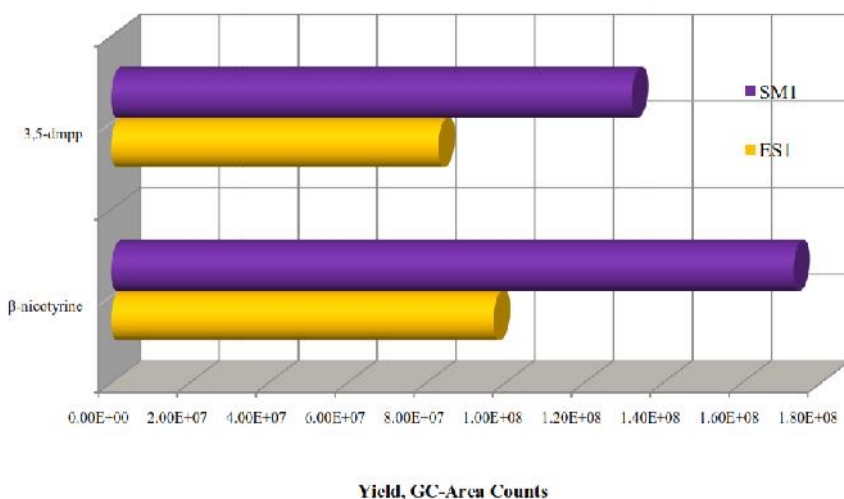

Fig. 3: Product yields of -nicotyrine and 3,5-dimethyl-1-phenylpyrazole (3,5-dmpp) for ES1 cigarette (pink) and SM1 (yellow).

It is evidently clear that of all the alkaloids determined in this study, nicotine was found in high concentrations in the two cigarettes in the entire pyrolysis temperature range. Nonetheless, while the maximum concentration of nicotine was noted at 400 ˚C (~ 8.0 x 10^8 GC-area counts) for ES1 cigarette, nicotine concentration peaked at ~500 ˚C (~2.7 x 10^8 GC-Area Counts) for SM1 cigarette. The ratio of nicotine in ES1 cigarette to that in SM1 cigarette was ~ 3 according to this study. This implies that ES1 cigarette contains about 3 times the amount of nicotine than SM1 cigarette. These results are remarkable and present the first intense study on two different commercial cigarettes coded ES1 and SM1 popularly sold around the world. Even more surprising is the fact that the maxima of the two cigarettes give a ratio of ~3. This validates the method of analysis used in this

investigation because virtually most of the reaction products of most biomass materials including tobacco peak between 300 and 500 ˚C [20,26]. From Fig. 2, it can be observed that whereas pyridine is the key product of ES1 cigarette, the other alkaloids (-nicotyrine and 3,5-dimethyl-1-phenylpyrazole, and pyrrole) have comparable concentrations in the two cigarettes under investigation. For instance in SM1 the total pyrrole concentration in the whole temperature range was found to be ~ 2.0 x 10^8 whereas in ES1 the total pyrrole concentration was found to be ~1.5 x 10^8 in the same temperature range. Nevertheless, the evolution of nicotine from ES1 is significantly high even at low temperatures (300 ˚C) as can be observed in Fig. 2. On the contrary, nicotine production from SM1 cigarette only becomes significant above 300 ˚C. In order to have

208

a clear overview of variations in concentrations between the other alkaloids explored in this work in the entire pyrolysis temperature range, Fig.3 is presented.

Clearly, SM1 cigarette yields significantly high concentrations of -nicotyrine and 3,5-dimethyl-1-phenylpyrazole in the whole pyrolysis range in comparison to ES1 cigarette (cf. Fig. 3). This contrasts sharply with the high yields of nicotine and pyridine noted in ES1. Based on these data alone, it can be noted that cigarette ES1 is very addictive considering the high levels of nicotine it produces during smoking and possibly the 'darling' of most cigarette smokers.

The overlay chromatograms indicating the identification of alkaloid reaction products explored in this work is presented in Fig. 4. The compounds numbered *a* and *b* represent -nicotyrine and 3,5-dimethyl-1-phenylpyrazole respectively as presented in Fig. 1, *vide supra*. It may be attractive to examine some of the other prominent peaks shown in the Fig. 4 but the principal focus of this study was to investigate the major tobacco alkaloids in a more thorough manner. The other reactions products which are mainly oxygenated compounds and aromatics will be reported in subsequent articles.
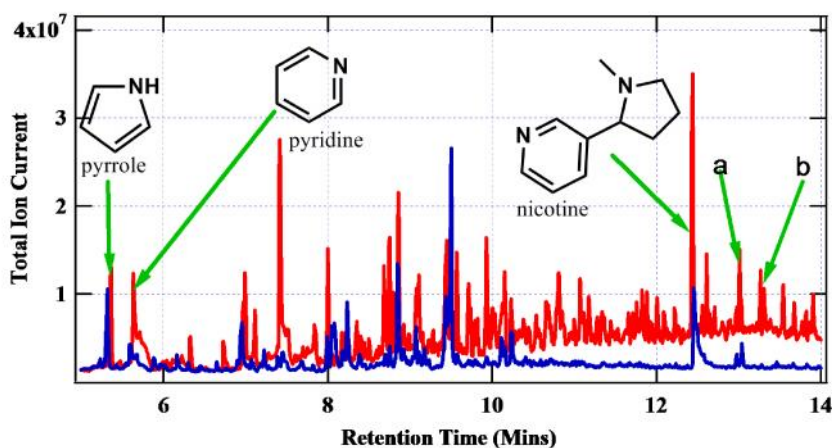

Fig. 4: Overlapping chromatograms for ES1 (red line) and SM1 (blue line) at 300 °C.

The proposed free radical formation from the thermal degradation of nicotine

Quantum mechanical calculations are fundamental in predicting new insights on feasible mechanisms on the thermal degradation of environmental pollutants. Figure 5 shows the use of various basis sets for formation of different radicals from the thermal degradation of nicotine. It is evident that there are some slight differences between various basis sets. The most consistent basis set chosen for this investigation is the 6-31G which appears suitable for the tobacco alkaloids under investigation.
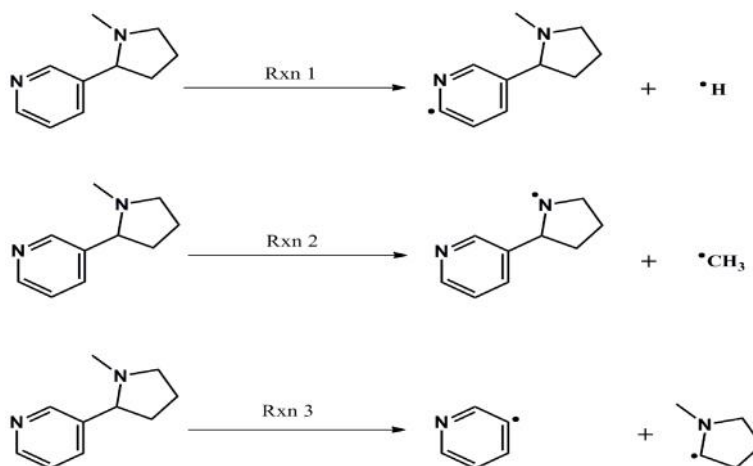
Scheme 1: The formation of various radicals from the thermal degradation of nicotine

Scheme 1, *vide supra* depicts the formation of various radicals in the proposed thermal degradation of nicotine in high temperature cigarette smoking. Clearly, reaction 3 proceeds with a lower energy in comparison to reactions 1 and 2. Reaction 3 therefore is a very important reaction because it leads to the formation of intermediates which can transform to other combustion by-products including pyridine (when pyridinyl radical reacts with H radical in the combustion system) or methylated pyrrolidine when pyrrodinyl radical reacts with H radical. Nonetheless, reactions of the free radical in reaction 3 with methyl radical to form 3-methyl pyridine is known but according to literature, the reactivity of H radical occurs by several magnitudes in comparison to the methyl radical [27,28]. This corroborates our experimental investigation in this study in which low yields of 3-methyl pyridine and aniline were detected. Pyrrole however, was reported in high yields in this study (Fig. 4) and may be attributed to the scission of the phenyl C-C linkage in -nicotyrine and possible other pyrosynthetic reactions during tobacco burning. The formation of free radicals and transient intermediates is considered the major reaction in tobacco burning. Free radicals are responsible for severe health conditions such as cardiac arrest, oxidative stress, tumours, and cancer related illnesses therefore understanding the energetics of these species are fundamental in demystifying cigarette smoking [29,30].
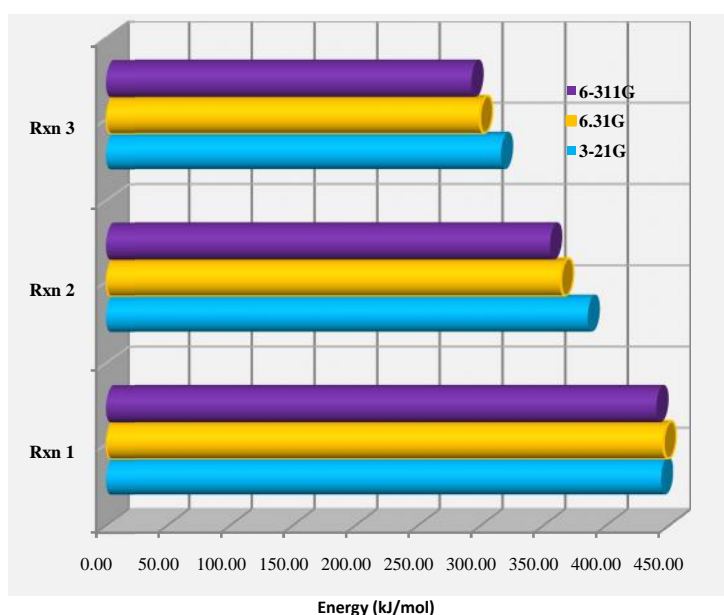

Figure 5: A plot of enthalpy change for reactions 1-3 (scheme 1) at various basis sets

Based on the thermodynamic data presented in Fig. 5, it is apparent that reactions 1 and 2 proceed with high energy and therefore not the major mechanistic pathways for the thermal decomposition of nicotine. A detailed mechanistic studies of -nicotyrine and 3,5-dimethyl-1-phenylpyrazole will be treated thoroughly in our next article from a theoretical perspective.

The toxicological consequences of cigarette smoking
There is no doubt that inhaled toxicants such as alkaloids in cigarette smoke can cause both irreversible alterations to the DNA and serious variations in the genetic landscape which include changes in the DNA methylation and chromatin alteration state [31,32]. Clearly, from this study, alkaloids and their corresponding free radicals are potential candidates for diseases that are believed to comprise genetic and epigenetic perturbations such as lung cancer, chronic obstructive pulmonary disease (COPD), and cardiovascular disease (CVD), all of which are strongly linked epidemiologically to cigarette smoking [31]. Lung cancer development involves various genomic aberrations, such as point mutations, deleterious effects, and gene amplifications[31]. Direct DNA damage by cigarette toxicants including nicotine, pyrrole, and pyridine has been linked to cardiovascular disease [31,32]. Additionally,

Reproductive function and fertility are thought to be compromised by behaviors such as cigarette smoking[2,32]. Although very little information is available in literature on the effects of -nicotyrine and 3,5-dimethylpyrazole, it is evident from this study that their molecular nature as well as their intermediate radicals may pose critical impacts to the biological structures of cigarette smokers. The molecular structure of nicotine and other alkaloid related compounds investigated in this work may covalently bond to the DNA, lipids, nuclei acids, and body cells before metabolizing to harmful by-products that are potentially risk to the human health.

CONCLUSION:

It was established in this study that most of the alkaloids were evolved between 400 and 500°C. Clearly, this is a region that should be avoided in the design of modern cigarettes because most organic toxics are released in this temperature range. Although cigarette research has dominated critical discussions in addiction and inhalation science with no conclusive remedy on sight, this study has presented interesting findings that may assist cigarette manufacturers to design cigarettes that can be smoked at lower temperatures and thereby avoid inhaling high levels of tobacco toxins usually smoked at high temperature smoking regimes. Therefore, cigarettes that can be smoked at a lower temperature would be beneficial to the general cigarette smoking community. Tobacco additives which may results in increased levels of organic toxins must be regulated. Evidently from this study, the commercial cigarette ES1 is very addictive considering the high levels of nicotine it emits during smoking.

REFERENCES:

1   Anand, PEA. Cancer is a Preventable Disease that Requires Major Lifestyle Changes. **Pharmaceutical Research.**(25); 2008: 2097-2116.
2   Lisko, et al. Application of GC-MS/MS for the Analysis of Tobacco Alkaloids in Cigarette Filler and Various Tobacco Species. **Analytical Chemistry.**85 (6); 2013: 3380-3384.
3   Wang, Z. Religious involvement and tobacco use in mainland China: a preliminary study. **BMC Public Health**.15;2015.
4   Lockman, PR, et al. Brain uptake kinetics of nicotine and cotinine after chronic nicotine exposure. **The Journal of Pharmacology and Experimental Therapeutics.**314(2); 2005: 216-230.
5   William, et al. Cigarette smoking in China: public health, science, and policy. **Reviews on Environmental Health.**27;2012: 43–49.
6   Mendelsohn, C. Nicotine dependence: Why is it so hard to quit? **Medicine Today.**12;2011:35-40.
7   Digard, H, et al. Determination of Nicotine Absorption from Multiple Tobacco Products and Nicotine Gum. **Nicotine and Tobacco Research.**(15); 2013: 255-261.
8   Bono,et al. Tobacco smoke and formation of N-(2-hydroxyethyl)valine in human hemoglobin. **Archives of Environmental Health.**57;2002: 416-421.
9   Merckel C. and Pragst, F. Tobacco additives in cigarettes - Intended purpose and potential of danger. **Journal of Consumer Protection and Food Safety.**(2);2007: 287-301.
10 Cappelleri,et al. Revealing the multidimensional framework of the Minnesota nicotine withdrawal scale. **Current Medical Research and Opinion.** 21; 2005: 749-760.
11 Benowitz, N. Neurobiology of Nicotine Addiction: Implications for Smoking Cessation Treatment. **The American Journal of Medicine.**121;2008: 3-10.
12 Shiffman, et al. Reduction of abstinence-induced withdrawal and craving using high-dose nicotine replacement therapy. **Psychopharmacology.**184; 2006: 637–644.
13 Anderson, et al. Treating tobacco use and dependence: an evidence-based clinical practice guideline for tobacco cessation. **Chest Journal.**121; 2002: 932-941.
14 Wetter, et al. Gender Differences in Smoking Cessation. **Journal of Consulting and Clinical Psychology.**67; 1999: 555-562.
15 Hesami, et al. Severity of Nicotine Withdrawal Symptoms after Smoking Cessation. **Tanaffos Journal.**9;2010: 42-47.
16 Stephen, SH. Lung carcinogenesis by tobacco smoke. **International Journal of Cancer.**131(12); 2012: 2724-2732.
17 Siegel, et al. Cancer statistics. **CA Caner J Clin.**62; 2012: 10-29.
18 Zhou, et al. The pyrolysis of cigarette paper under the conditions that simulate cigarette smouldering and puffing. **Journal of Thermal Analysis and Calorimetry.**104(3); 2011: 1097-1106.
19 Hecht, SS. Carcinogenicity studies of inhaled cigarette smoke in laboratory animals: old and new. **Carcinogenesis.**26(14); 2005: 88-92.
20 Kibet,et al. Molecular Products and Radicals from Pyrolysis of Lignin. **Environmental Science and Technology,**46(23): 2012: 2994-13001.
21 Zhang, et al. Atmospheric oxidation mechanism of naphthalene initiated by OH radical. A theoretical study. **Phys. Chem. Chem. Phys.**14; 2010: 2645–2650.
22 Boese, AD. Density Functional Theory and Hydrogen Bonds: Are We There Yet? **ChemPhysChem.**16; 2015; 978-985.
23 Ben, HX. and Ragauskas, AJ. NMR Characterization of Pyrolysis Oils from Kraft Lignin. **Energy and Fuels.**25 (5); 2011: 2322-2332.
24 Kibet, et al. Molecular Products from the Thermal Degradation of Glutamic Acid. **Journal of Agricultural and Food Chemistry.**4; 2013: 178-184.
25 Kibet, et al. Phenols from pyrolysis and co-pyrolysis of tobacco biomass components. **Chemosphere.**138; 2015: 259-265.
26 Sharma,et al. Characterization of chars from pyrolysis of lignin. **Fuel.**83(11-12);2004: 1469-1482.
27 Kibet, et al. Molecular products from the pyrolysis and oxidative pyrolysis of tyrosine. **Chemosphere.**91; 2013: 1026-1034.
28 Khachatryan, et al. Development of expanded and core kinetic models for the gas phase formation of dioxins from chlorinated phenols. **Chemosphere.** 52(4);2003: 695-708
29 Maskos, et al. Formation of the persistent primary radicals from the pyrolysis of tobacco. **Energy and Fuels.**22(2), 2008: 1027-1033.
30 Maskos, et al. Precursors of radicals in tobacco smoke and the role of particulate matter in forming and stabilizing radicals. **Energy and Fuels.**19(6); 2005: 2466-2473.
31 Talikka,et al. Genomic impact of cigarette smoke, with application to three smoking-related diseases. **Critical Reviews in Toxicology.**42(10);2012: 877–889
32 Sadeu, et al. Alcohol, drugs, caffeine, tobacco, and environmental contaminant exposure: Reproductive health consequences and clinical implications. **Critical Reviews in Toxicology.**40 (7);2010: 633–652.

RESEARCH ARTICLE

Synthesis and Characterization of Some Crown Ether Complexes of Tl(I) Ion

Rajeev Ranjan*, Poonam Bhardwaj, Seema Chitlangia, Jitesh Kumar Nayak
PG Department of Chemistry, Ranchi College, Ranchi-834008
*Corresponding Author E-mail: **rajeevran7@yahoo.com**

ABSTRACT:
The affinity of crown ethers for metal ion is strongly dependent on the size of the ring of the crown ether. The crown ether-metal ion binding is enhanced in the absence of non-coplanar donor oxygen atoms and electron withdrawing substituents in the crown ether skeleton. The study of absorption of radio frequency radiation by a magnetic nucleus provides useful information regarding structure of a number of organic and inorganic compounds. Small changes were observed in the chemical shift of 1-H in 15C5, 18C6 and, 1-H as well as 2-H, in dibenzo18C6. After formation of the [Metal-Crown ether]Ligand complex, the proton chemical shift $\delta(-CH_2-O-)$ shows significant downfield shifts [$\delta(-CH_2-O-)= 0.08\text{-}0.25$ ppm], indicating metal-ligand bond formation. The degree of downfield shift shows the relative strength of the complexes. The ^{1}H-NMR spectrum of dibenzo18C6 shows peaks at, $\delta_1=3.9\text{-}4.1$ ppm, (16H, 8 $-CH_2O-$), $\delta_2=6.8\text{-}7.0$ ppm, (8H, aryl $-CH-$), in $CDCl_3$. The shift of $-CH_2-$ signals in complexes from free crown ether unambiguously suggested the coordination of crown ether oxygen of 15C5, 18C6 as well as dibenzo18C6 with thallium ion.

The present paper describes the preparation and characterization of some Tl(I) complexes with 1,4,7,10,13,-pentaoxacyclopentadecane (15C5), 1,4,7,10,13,16,-hexaoxacyclooctadecane (18C6) and 2,3,11,12-dibenzo-1,4,7,10,13,16,-hexaoxacyclooctadeca-2,11-diene (dibenzo18C6), having five and six donar oxygen atoms respectively. The metal salts used for complexation are salts of nitrophenols. Products were isolated from thallium salts of all the three monoionic ligands, 2-nitrophenol (ONPH), 2,4-dinitrophenol (DNPH) and 2,4,6-trinitrophenol (TNPH) and were chromotographed using TLC. The bonding patterns of complexes were suggested from the studies of elemental analysis, molar conductivity, IR, UV-Vis and ^{1}H-NMR spectral analysis.

KEYWORDS: 15C5, 18C6, ONPH, DNPH, TNPH.

INTRODUCTION:
Crown ethers have the unusual property to form stable complexes with metal ions. This exceptional stability has been attributed to the close fitting of the metal ion in the hole at the centre of the ligand. The crown ethers show selectivity among the suitable metal ions in forming complexes. The metal crown binding is enhanced in the absence of non-coplanar donor oxygen atoms and electron withdrawing substituents within the crown. The affinity of crown for alkali and alkaline earth metal ion is strongly dependent on the size of the ring opening in the crown. Numerous theoretical and experimental studies of

the crown-cation interaction have been performed. Theoretical studies employing abinitio,[1-4] semiempirical[5] and molecular mechanics methods[6-15] have been focused on the structure and selectivity of crown ethers towards metal ions. Although in many cases the results of the calculations have qualitatively observed relative stabilities of crown cation complexes, there is sometimes a large discrepancy between the calculated values of binding energy and the experimental binding enthalpy.[16]

MATERIALS AND METHODS:

All chemicals used were of S. Aldrich / E. Merck, A.R. grade. The metal contents were estimated by flame photometric method. The melting point of the synthesized compounds, were determined on electrical tempo T-1150 melting point apparatus. Molar conductivities of the compounds were measured using Systronic conductivity meter-306. The conductivities of the compounds were measured at the concentration 10^{-3} M in methanol solvent at $30(\pm0.5)^0$C. IR spectra were recorded by Perkin Elmer RX1 (4000-450 cm^{-1}). UV-visible spectral data were recorded through Systronic double beam spectrophotometer-2203 (600-200 nm). The ^{1}H–NMR spectra of ligand and crown ether complexes were recorded in CDCl$_3$ by Bruker DRX-300.

Experimental :
Preparation of thallium salt of nitrophenols; Tl(ONP), Tl(DNP) and Tl(TNP) :

About 0.02 mol of appropriate nitrophenol was taken in a conical flask and dissolved in 50 ml of dry ethanol with constant stirring with the help of glass rod. Further 0.02 mol of metal hydroxide was dissolved in ethanol and was slowly added to the alcoholic solution of nitrophenol with constant stirring. The mixture was continuously refluxed on hot plate equipped with magnetic stirrer for 50 minutes and the temperature was maintained at 78^0C. The solution in conical flask was corked and kept standed. On cooling this solution solid crystalline product began to precipitate slowly. Product was filtered, washed with absolute ethanol and dried in an electric oven at 80^0C.

Preparation of 15C5, 18C6 and dibenzo18C6 ether:

Preparation of crown ethers which may work as a strong complexing host molecule was one of the important part of this research work. These were prepared by the synthetic methods as reported in literature.[17-18]
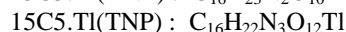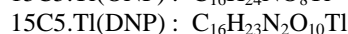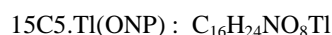
Table 1.1 Physical properties of thallium salts

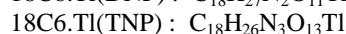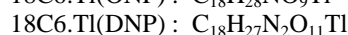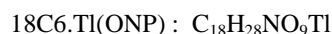| Compound	Colour	Melting point (^{0}C)
Tl(ONP)	Light yellow	275 d
Tl(DNP)	Bright yellow	270 d
Tl(TNP)	Light orange	270 e

d – decomposition temp, e – explosion temp

Preparation of adducts of 15-crown-5 and 18-crown-6 ether with thallium salts of 2-nitrophenol, 2,4-dinitrophenol and 2,4,6-trinitrophenol.

The dried organic salt (0.002 mol) was suspended in 50 ml dry methanol and heated it with constant stirring to get a clear solution. Stoichiometric proportion of 15-crown-5 ether (0.002 mol) was added in this solution. This reaction mixture was refluxed on a hot plate equipped with magnetic stirrer at 50-55^{0}C. A clear solution was formed. It was filtered and concentrated to half of its bulk. On cooling this solution, solid crystalline product began to precipitate. The product was separated and allowed to stand overnight then filtered on a buchner funnel. The compound was washed with a little cold dry methanol and dried over KOH desiccator.

15C5.Tl(ONP) : C$_{16}$H$_{24}$NO$_8$Tl
15C5.Tl(DNP) : C$_{16}$H$_{23}$N$_2$O$_{10}$Tl
15C5.Tl(TNP) : C$_{16}$H$_{22}$N$_3$O$_{12}$Tl

Similarly, in the preparation of adducts of 18-crown-6, same amount of appropriate dried thallium salt was refluxed with 0.528 gm (0.002 mol) of 18-crown-6 ether.

18C6.Tl(ONP) : C$_{18}$H$_{28}$NO$_9$Tl
18C6.Tl(DNP) : C$_{18}$H$_{27}$N$_2$O$_{11}$Tl
18C6.Tl(TNP) : C$_{18}$H$_{26}$N$_3$O$_{13}$Tl

Preparation of adducts of dibenzo18-crown-6 with thallium salt of 2,4-dinitrophenol and 2,4,6-trinitrophenol.

The dried thallium salt (0.002 mol) was suspended in 50 ml dry methanol in a conical flask and heated it with stoichiometric proportion of dibenzo18-crown-6 ether (0.002 mol, 0.72 gm). The reactant mixture was refluxed on a hot plate equipped with magnetic stirrer at 50-55^{0}C. A clear solution was formed. On concentrating and cooling this solution, solid crystalline product began to precipitate. The product was separated and allowed to stand overnight and again filtered on a buchner funnel. The compound was washed with a little cold dry methanol and dried over KOH desiccator.

DB18C6.Tl(DNP) : C$_{26}$H$_{27}$N$_2$O$_{11}$Tl
DB18C6.Tl(TNP) : C$_{26}$H$_{26}$N$_3$O$_{13}$Tl
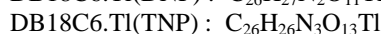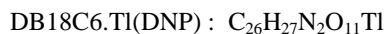
Table 1.2 Prominent IR bands of thallium complexes (in cm^{-1})

Compound	ϵ_s(C–H)$_{bending}$, ϵ_{as}(–CH$_2$–)$_{bending}$	ϵ(N=O)$_{str\ in}$ C–NO$_2$
15C5.Tl(ONP)	1499, 1331	1220
15C5.Tl(DNP)	1477, 1348	1219
15C5.Tl(TNP)	1436, 1327	1219
18C6.Tl(ONP)	1501, 1354	1250
18C6.Tl(DNP)	1448, 1356	1220
18C6.Tl(TNP)	1471, 1353	1249
DB18C6.Tl(DNP)	1435, 1325	1219
DB18C6.Tl(TNP)	1454, 1363	1215

Table 1.3 Prominent IR bands of thallium complexes (in cm^{-1})

Compound	ϵ_{as} (C>O>C)	ϵ_1 (>NO$_2$), ϵ_3 (>NO$_2$)	ϵ (C>H) Phenolic out of Plane
15C5.Tl(ONP)	1122	1606, 852	771
15C5.Tl(DNP)	1219	1630, 862	772
15C5.Tl(TNP)	1086	1623, 870	772
18C6.Tl(ONP)	1020	1604, 875	763
18C6.Tl(DNP)	1018	1601, 860	768
18C6.Tl(TNP)	1108	1631, 836	767
DB18C6.Tl(DNP)	1130	1626, 870	772
DB18C6.Tl(TNP)	1057	1631, 845	766

Table 1.4- Prominent far-IR bands of thallium complexes (in cm^{-1})

Compound	ϵ(M–O) / ϵ(M–O$_{crown}$)
15C5.Tl(ONP)	535, 560
15C5.Tl(DNP)	510, 550
15C5.Tl(TNP)	482, 545
18C6.Tl(ONP)	533, 562
18C6.Tl(DNP)	528
18C6.Tl(TNP)	524, 584
DB18C6.Tl(DNP)	529, 570, 590
DB18C6.Tl(TNP)	475, 530, 580

RESULTS AND DISCUSSIONS :

IR study :

The free nitro groups of nitrophenols display –NO$_2$, ν_{as} and ν_s stretching around 1620±15 cm^{-1}, 1260±30 cm^{-1}. The –NO$_2$ bending band is located at 840±20 cm^{-1} which has been found to be affected and shifted to lower frequency by 10–15 cm^{-1} on bond formation. The phenyl group in all nitrophenols and 8-hydroxyquinoline display phenyl (C=C) and (C–H) skeletal vibration at four positions in finger print region. The first phenyl group skeletal vibration is observed at 1590–1620 cm^{-1} and second at about 1510±15 cm^{-1}. The third and fourth band is observed near 1280±10 cm^{-1}. The IR band observed near 740–780 cm^{-1} is attributed to phenyl ring (C–H) out of plane bending band. The absorption at about 1110 cm^{-1} is attributed to phenolic (C–O) stretching band. In present study all nitrophenols display ν(O–H) frequency as broad band in the region 3140–3320 cm^{-1} and ν(C–O) near 1120±10 cm^{-1}. The ν(O–H) disappears in thallium salts and ν(C–O) band shifted to higher frequency due to acquiring higher (C–O) bond order on deprotonation. This increase is attributed to bonding of phenolic oxygens (C–O) in all complexes.

The stretching bands of –NO$_2$ in Tl(ONP), Tl(DNP) and Tl(TNP) is at around 1605 cm^{-1}, 1620±2 cm^{-1} and 1640–1645 cm^{-1}. These vibrations shifted to lower frequency in complexes. The ν(NO$_2$) located near 840±15 cm^{-1} also shifted to lower vibrational frequency in complexes. The crown ethers display ν(CH$_2$) stretching vibrations at 2925±10 cm^{-1} and these are little affected on bonding with metal ions. The crown ethers in uncoordinated state display ν(C-O-C) stretching vibration band near 1115±10 cm^{-1}. This ν(C-O-C) vibration band shifted to

lower frequency by 10 to 60 cm^{-1} in almost all compounds suggesting involvement of crown ether oxygen in bond formation with thallium ion. Some complexes are hygroscopic in nature and thus their IR spectrum displays a broad band of water molecules around 3350–3420 cm^{-1}, with maxima near 3405±10 cm^{-1}. In the far-IR region new bands, absent in the spectrum of the free ligands, are found in the 425-590 cm^{-1} region, which may be assigned to the ν(M–O$_{crown}$) stretching frequency. Thus IR studies of complexes unambiguously suggest bonding of thallium salts of nitrophenols with crown ether oxygen atoms.

^{1}H-NMR Study :

The ^{1}H-NMR spectrum of uncoordinated crown ethers and some adduct complexes of thallium ions provide effective information. The structural units of protons, phosphorus, fluorine, iodine and some other nucleus with I≠O, gives splitting of NMR signals at different energy and magnetic field region of radio frequency radiation. The ^{1}H-NMR signals are affected appreciably by type and environment of magnetic nucleus. The magnetic field that is experienced by the first nucleus is the effective sum of externally applied field after shielding electron and that owing to the second nucleus.
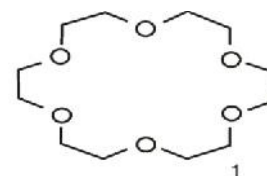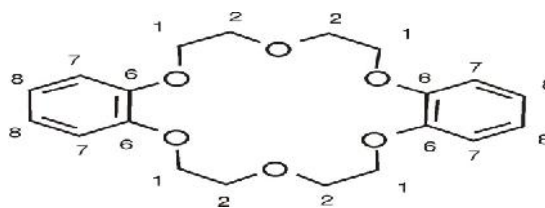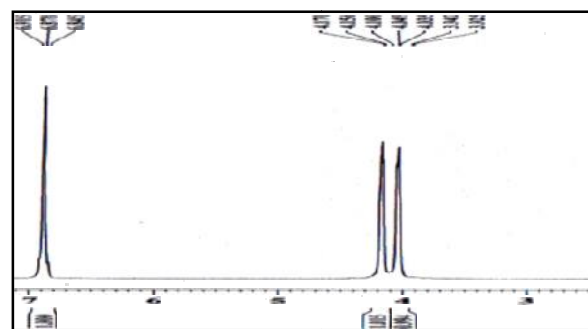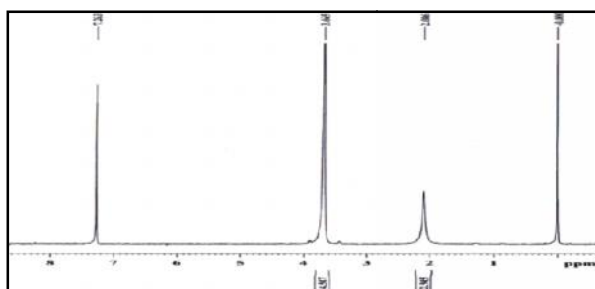

Fig 1.1 : 15-crown-5   Fig 1.2 : 18-crown-6
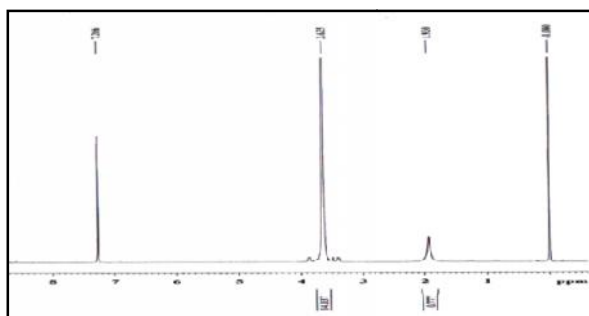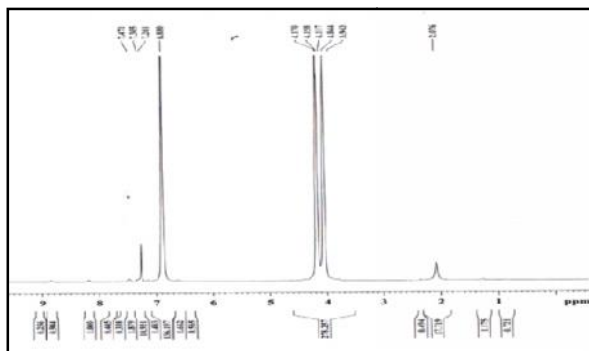

Fig 1.3 : Dibenzo18-crown-6

Fig 1.4 : ^{1}H-NMR of Dibenzo18-crown-6

Fig 1.5: ^{1}H-NMR of 18C6.Tl(TNP)

Fig 1.6: ^{1}H-NMR of 18C6.Tl(ONP)

Fig 1.7: ^{1}H-NMR of DB18C6.Tl(ONP)

^{1}H-NMR Chemical shift (u) for free crown ethers and synthesized complexes

Compound	u(1H)	u(2H)	u(7H, 8H)
15C5	3.621		
Na$^+$-15C5	3.627		
18C6	3.623		
Na$^+$-18C6	3.665		
DB18C6	3.925	4.035	6.8 – 7.0
Na$^+$-DB18C6	3.943	4.031	6.8 – 7.0

Small changes were observed in the chemical shift of 1H in 15C5, 18C6 and 1H as well as 2H in dibenzo18C6[19], which moved downfield upon complexation. The degree of downfield shift mirrored the relative strength of the complexes. The chemical shift variation indicates a possible change in the structure and/or electronic environment of 1H and 2H in these systems on complexation. Possible reasons for this downfield shift are the conformational change in the macrocyclic skeleton during complexation which could change the position of the aliphatic protons, the electric field effect of the metal cation in the complexes or change in bonding to adjacent atoms, which could affect the electron density on the hydrogen through the Fermi contact term.[20] Significant change in the –OCCO– dihedral angle upon complexation is probably a major contributor to the chemical shift in some complexes.

After formation of the [Metal-Crown ether]Ligand complex, the proton chemical shift of $\delta(-CH_2-O-)$ shows significant downfield shifts [$\delta(-CH_2-O-)$=0.08-0.25 ppm], indicating metal-ligand bond formation.[21] Thus coordination of ligand molecule with metal ion provides much information regarding bonding due to change of electron shielding effect, spin-spin coupling, spin-spin splitting pattern and extent of coupling constant(j). These values provide significant information about the change of magnetic environment of protons on bonding, and change in orientation of the molecules on the formation of new bond.

The proton NMR spectrum of dibenzene 18C6 polyether shows ^{1}H-NMR peaks δ = 3.9–4.1 ppm, (16H, 8 – CH_2O-), δ = 6.8–7.0 ppm (8H, aryl –CH–)[22-25] in $CDCl_3$. The shift of –CH$_2$– signals in complexes from free crown ether unambiguously suggested the coordination of crown ether oxygen of 15C5, 18C6 as well as dibenzo18C6 with thallium ion.

REFERENCES:
1. Hori K, Yamada H, Yamabe T, Tetrahedron, 39, (1983), 67
2. Ha YL, Chakraborty AK, J. Phys. Chem., 96, 6410, (1992)
3. Glendening ED, Feller D, Thompson MA, J. Am. Chem. Soc., 116, (1994), 10657
4. Rencsok R, Kaplan TA, Harrison JF, J. Phys. Chem., 92, (1993), 9758
5. Yamabe T, Hori K, Akagi K, Fukui K, Tetrahedron, 35, (1979), 1065
6. Hancock RD, Acc. Chem. Res., 23, (1990), 253
7. Hay BP, Rustad JR, Hostetler CJ, J. Am. Chem. Soc.,115, (1993), 11158
8. Mazor MH, McCammon JA, Lybrand TP, J. Am. Chem. Soc., 112, (1990), 4411
9. Wipff G, Weiner P, Kollman P, J. Am. Chem. Soc.,104, (1982), 3249
10. Dang LX, Kollman PA, J. Am. Chem. Soc. 112, (1990), 5716
11. Howard AE, Singh UC, Billeter M, Kollman PA, J. Am. Chem. Soc., 110, (1988), 6984,

12. Marrone TJ, Hartsough DS, Merz Jr. KM, J. Phys. Chem., 98, (1994), 1341
13. Ha YL, Charkaborty AK, J. Phys. Chem., 97, (1993), 11291
14. Ha YL, Charkaborty AK, J. Phys. Chem., 95, (1991), 10781
15. Leuwerink FTH, Harkema S, Briels WJ, Feil D, J. Comput. Chem., 14, (1993), 899
16. Thompson MA, Glendening ED, Feller D, J. Phys. Chem., 98, (1994), 10465
17. Pedersen CJ, *J. Am. Chem. Soc,* 89, 7017, 1967
18. Pedersen CJ, *J. Am. Chem. Soc,* 92, 386, 1970
19. Wilson MJ, Pethrick RA, Pugh D, Islam MS, J. Chem. Soc, Faraday Trans, 93, 11, (1997), 2097
20. Fulmer GR, Miller JMA, Sherden NH, Organometallics, 29, (2010), 2176
21. Lu T, Gan X, Tan M, Su H, Liu Y, Polyhedron, 12, (1993), 1055
22. Wilson MJ, Pethrick RA, Pugh D, Islam MS, J. Chem. Soc, Faraday Trans, 93, (1997), 387
23. Mojtaba S, Mohsen I, J. Solution. Chem, 37, (2008), 657
24. Noguchi H, Nagamatsu M, Yoshuo M, Bull. Chem. Soc. Jpn, 58, (1985), 1855,
25. Czech BP, Czech A, Knudser BE, Bartsch RA, Gazz. Chim. Ital, 117, (1987), 717

RESEARCH ARTICLE

Characterization of cyanobacterial toxins in Lake Naivasha, Kenya

D. N. Nyachiro[1], B. G. Ongarora[2]*, J. K. Kibet[1], N. K. Rono[1]
[1]Department of Chemistry, Egerton University P.O Box 536 - 20115, Egerton, Kenya
[2]Department of Chemistry, Dedan Kimathi University of Technology P.O Box 657 - 10100, Nyeri, Kenya
*Corresponding Author E-mail: **benson.ongarora@dkut.ac.ke**

ABSTRACT:
Microcystins are a class of cyanobacterial toxins largely found in water and are often responsible for poisoning animals as well as humans. A more recent scenario is the poisoning of domestic water supply system in Toledo (Ohio), USA. Consequently, water supply to the city had to be suspended for weeks in order for authorities to ascertain the commodity's safety before restoring supply. In Kenya, there have been very few studies on cyanotoxins and their adverse health effects in spite of the fact that cyanobacteria have been implicated in several poisoning episodes of humans and animals worldwide, occasioned by drinking of microcystin contaminated water. This paper therefore, reports data on the first identification and characterization of hepatotoxic microcystins in water samples of Lake Naivasha. Samples from the lake were investigated over a modest period of three months. The phytoplankton community was mainly dominated by the cyanobacterium *Microcystis aeruginosa*. The colour of the water samples was found to be 520 ± 91 ptco, while the conductivity was 234 ± 0.8 µs/cm and the total dissolved solids was 1035 ± 12 mg/L. Due to the high turbidity (59.0 ± 24 ntu), phytoplankton biomass was low, ranging between 1.5 and 8.2 mg L^{-1}. Using UV-Vis and HPLC techniques, the microcystin-LR and -RR were detected in all the water samples collected from the lake. HyperChem computational package was used to estimate the toxicity index of microcystin-RR based on the octanol-water partition coefficient and found to be 230 times more soluble in water than in octanol. Thus, microcyctin-RR is highly soluble in polar biological tissues which may result in cell injury, oxidative stress, and ultimately cancer. To the best of our knowledge, this is the first evidence of microcystins in Lake Naivasha.

INTRODUCTION:
Cyanobacterial toxins are the naturally produced poisons stored in the cells of certain species of cyanobacteria.[1] Very few cyanobacterial toxins have actually been isolated and characterized to date. One group of toxins produced and released by cyanobacteria are called *microcystins* because they were isolated from a cyanobacterium called *Microcystis aeruginosa*.

Microcystins are the most common of the cyanobacterial toxins found in water, as well as being the ones most often responsible for poisoning animals and humans who come into contact with toxic blooms.[1] Microcystins are extremely stable in water because of their chemical structure, which means they can survive in both warm and cold water and can tolerate radical changes in water chemistry, including pH. So far, scientists have found about 50 different kinds of microcystins. One of them, microcystin-LR, appears to be one of the microcystins most commonly identified in water supplies around the world. For this reason, most research in this area has focused on this particular toxin.

Microcystins have been described and detected in several cyanobacteria genera. These include *Anabaena*, *Microcystis Oscillatoria, Planktothrix*.[2-5] Worldwide, the nearly all cyanotoxin encountered in fresh and brackish waters are the cyclic peptides known as microcystin.[6]

Cyanobacteria toxins fall into various categories. Some are known to attack the liver (hepatotoxins) or the nervous system (neurotoxins); others simply irritate the skin. People swimming in dense *Microcystis* blooms have experienced irritation such as skin rashes, burns, and blistering of the mouth. Ingestion or inhalation of water containing dense bloom material may cause vomiting, nausea, headaches, diarrhea, pneumonia, and fever. Ingestion of significant levels of the toxin microcystin can cause liver damage and dysfunction in humans and animals.

Microcystins have been described as potent liver toxins[7], and in chronic cases are known to promote or initiate the growth of tumours. In other cases, they have been found to inhibit protein phosphatase activity.[8] They are synthesized non-ribosomally and by thiotemplate mechanisms. In Kenya, there have been few studies on cyanobacteria, cyanotoxins and possible adverse public health effects on humans. This is despite the established knowledge that cyanobacteria have been implicated in several poisoning episodes of humans and animals worldwide through drinking water.

In Bahia, Brazil, *Anabaena* and *Microcystis* (cyanobacterial toxins) from drinking water resulted in the death of 88 children from over 2000 cases of gastroenteritis over a period of 42 days.[9] Another case of human mortality occurred in Brazil, at a haemodialysis clinic where patients were treated with drinking water contaminated with cyanotoxins.[10] Over 50 people died in this incident. Examination of the phytoplankton in the reservoir showed the dominance of the cyanobacteria *Microcystis*, *Anabaena* and *Anabaenopsis*. A more recent scenario is the poisoning of domestic water supply system in Toledo (Ohio), USA. Consequently, water supply to the city had to be suspended for weeks in order for authorities to ascertain the commodity's safety before restoring supply. In this paper, we report the presence of microcystins in Lake Naivasha.

MATERIALS AND METHODOLOGY:
All reagents used in the study were of analytical grade. The reagents were purchased from commercial suppliers and used directly without further purification. The samples were collected from Lake Naivasha (Nakuru County, Kenya) and filtered through cartridge within four hours of collection for analysis. Solid phase extraction cartridges, Sep-pak© light tc18, were obtained from Waters Corporation Milford, Massachusetts USA.

The Brannan 76 mm pH meter (UK) and UV-Vis (1800 240V Shimadzu) were used in analysis of samples, in addition to HPLC and computation techniques.

In order to analyze the concentration of microcystin, water samples were concentrated according to the literature procedure.[11] Preliminary studies of microcystins were carried out using UV spectra (200-300 nm) and confirmed using HPLC-PDA retention times reported in literature.

RESULTS AND DISCUSSION:
The physico-chemical properties of the water samples were analyzed and the results are recorded in Table 1. The colour of the water samples ranged between 520 ± 91 ptco, signaling low transparency throughout the period. The conductivity was 234 ± 0.8 µs/cm and the total dissolved solids were found to be 1035 ± 12 mg/L. The pH of the lake remained slightly alkaline, averaging about 7.6 for the period under study. Due to the high turbidity (59.0 ± 24 ntu), phytoplankton biomass was low, ranging between 1.5 and 8.2 mg L^{-1}.

Table 1: Physico-chemical properties of Lake Naivasha

Parameter	Jan	Feb	March
Water temperature (°C)	26.1	26.3	26.7
pH	7.41	7.88	7.62
Turbidity (ntu)	69.0	59.4	44.6
TDS	1035	1054	1025
Colour (ptco)	377	306	360
Conductivity (µs/cm)	235	236	234

Using UV-Vis and HPLC techniques, the microcystin-LR and -RR were detected in all the water samples collected from the lake. Microcystin-LR, and microcystin-RR were identified based on their retention times, 11.45 and 5.01 respectively as shown in Figure 1.[12]
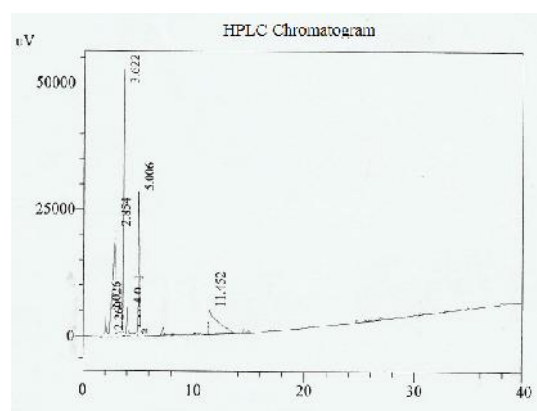

Fig. 1. HPLC-PDA chromatogram of water from Lake Naivasha.

Log P value, which is usually calculated as the octanol-water partion coefficient, is a measure of the toxicity index of a molecule. In this case, microcystin-RR is approximately 230 times more soluble in water than in octanol (Table 2). Thus, microcystin-RR (Figures 2A and 2B) is highly hydrophilic and may react with polar biological tissues, causing extensive cell injury, oxidative stress, and ultimately cancer. Lipophilicity, as measured by the base 10 logarithm of the octanol-water partition coefficient (P) and denoted as log *P*, is included as a possible contributory factor to the toxicity. Log *P* correlates with a number of biological activities including *in vitro* mutagenicity and carcinogenicity.[12] Lipophilic compounds including microcystins can cross biological barriers which contain lipids, for example, cell or microsomal membranes and skin stratum.[13,14] Therefore, log *P* influences metabolic fate, intrinsic biological activity and the biological transport properties of chemicals.[14]

Table 2. Molecular properties of microcystin-RR

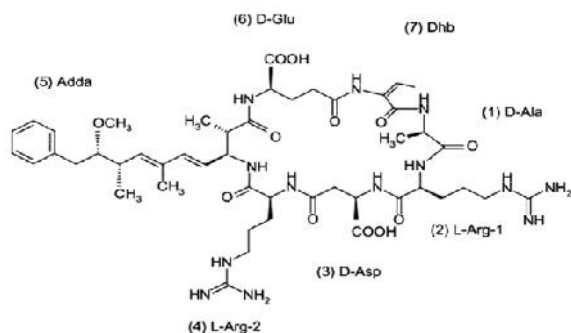| Name	Log P	P	Molar mass (a.m.u)
Microcystin-RR	-2.36	0.004	1024.19

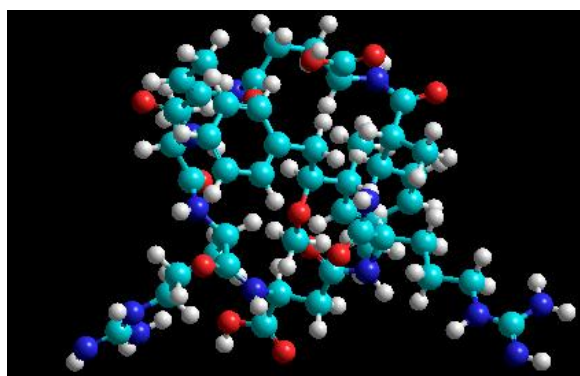**Fig. 2A**: Molecular structure of microcystin-RR

Fig. 2B: The modeled structure of microcystin-RR

Our study revealed that cyanobacteria in Lake Naivasha produce microcystins. Microcystin-LR and microcystin-RR were found in varying amounts. Worldwide, more than 60 structural variants of microcystins have been isolated.[9,15] Estimated as microcystin concentration per litre of lake water, the concentrations of microcystins-LR equivalents in Lake Naivasha range from 0.06 to 1.3 µg MC equ L^{-1} lake water. These values are within the safe level of Health Canada of 1.5 µg MC equ L^{-1}.[9,16] Although the levels are acceptable, the situation may change especially after Kenya changed its status from low-income economy to middle-income economy. There is expected to be accelerated use of fertilizers within Naivasha area in order to feed its rising population and this may lead to growth of algal blooms. This will raise the concentrations to levels that can have serious ecological impact on aquatic food web of the lake and cause serious health problems.[15,17,18]

CONCLUSION:
The impact of microcystins on the food web of Lake Naivasha, domestic animals and on public health in the region has so far not been investigated. The lake water is used by locals as drinking water for households and domestic animals. In some cases, the water is either used without treatment or treated with aluminium sulphate to settle down the sediments. To minimize harmful effects on consumers, we recommend that the water of Lake Naivasha should be pretreated in order to remove the any cyanobacterial toxins that may pose health hazard to the consumers. Further research also needs to be carried out in order to provide an up to date data on microcystins at Lake Naivasha and other water bodies in Kenya.

REFERENCES:
1 Yoo RS. Cyanobacterial (blue-green algal) toxins: a resource guide. **American Water Works Association, USA**. 1995.
2 Botes DP *et al*. The structure of cyanoginosin-LA, a cyclic heptapeptide toxin from the cyanobacterium Microcystis aeruginosa. **Journal of the Chemical Society**. 1; 1984: 2311-2318.
3 Brittain S *et al*. Isolation and characterization of microcystins from a River Nile strain of Oscillatoria tenuis Agardh ex Gomont. **Toxicon**. 38; 2000: 1759-1771.
4 Meriluoto J *et al*. Structure and toxicity of a peptide hepatotoxin from the cyanobacterium Oscillatoria agardhii. **Toxicon**. 27; 1989: 1021-1034.
5 Krishnamurthy T, Carmichael W and Sarver E. Toxic peptides from freshwater cyanobacteria (blue-green algae). I. Isolation, purification and characterization of peptides from Microcystis aeruginosa and Anabaena flos-aquae. **Toxicon**. 24(9); 1986: 865-873.
6 McElhiney J and Lawton LA. Detection of the cyanobacterial hepatotoxins microcystins. **Toxicology and applied pharmacology**. 203; 2005: 219-230.
7 Falconer IR *et al*. Toxicity of the blue-green alga (cyanobacterium) Microcystis aeruginosa in drinking water to growing pigs, as an animal model for human injury and risk assessment. **Environmental Toxicology and Water Quality**. 9; 1994: 131-139.

8   Yoshizawa S *et al.* Inhibition of protein phosphatases by microcystis and nodularin associated with hepatotoxicity. **Journal of Cancer Research and Clinical Oncology**. 116; 1990: 609-614.

9   Ballot A *et al.* Cyanobacterial toxins in lake Baringo, Kenya. **Limnologica-Ecology and Management of Inland Waters**. 33; 2003: 2-9.

10 Jochimsen EM *et al.* Liver failure and death after exposure to microcystins at a hemodialysis center in Brazil. **New England Journal of Medicine**. 338; 1998: 873-878.

11 Chorus I and Bartram B. Toxic Cyanobacteria in Water: A guide to their public health consequences, monitoring and management. **St Edmundsbury Press, Great Britain**. WHO, 1999.

12 DeLorenzo ME and Fulton MH. Water quality and harmful algae in Southeastern coastal stormwater ponds. **NOAA Technical Memorandum NOS NCCOS 93**. 2009: 1-27.

13 Debnath AK. *et al*. Importance of the hydrophobic interaction in the mutagenicity of organic compounds. **Mutation Research**. 305; 19994: 63-72.

14 Smith CJ and Hansch C. The relative toxicity of compounds in mainstream cigarette smoke condensate. **Food and Chemical Toxicology**. 38; 2000: 637-646.

15 Codd GA *et al.* Cyanobacterial toxins, exposure routes and human health. **European Journal of Phycology**. 34; 1999: 405-415.

16 WHO Guidelines for drinking-water quality. Vol. 2, Health criteria and other supporting information: addendum. **WHO**, 1998.

17 Chorus I. Cyanotoxins: Occurrence, Causes, Consequences. **Springer, Berlin Heidelberg**. 2001.

18 Carmichael WW and Falconer IR. Diseases related to freshwater blue-green algal toxins, and control measures. Algal toxins in seaa food and drinking water. Falconer IR ed. **Academic Press Limited, London**. 1993: 187-209.

www.ajrconline.org

RESEARCH ARTICLE

S,N-containing redox-polymers on the basis of allylamine

E.E.Ergozhin[1], [1]B.A.Mukhitdinova[1]*, N.P.Bessonova[2], T.K.Chalov[1], A.I.Nikitina[1]
[1]ISC, Institute of Chemical Sciences Named After A.B. Bekturov, 106, Sh. Ualichanov Str.,050010 Almaty, Republic of Kazakhstan
[2]ISC, Research Physical and Chemical Institute Named After L. Ya. Karpov, 3-1/12 by-str. Obucha, 105064, Moscow, Russia
*Corresponding Author E-mail: **mukhitdinovab@mail.ru**

ABSTRACT:
S,N-containing redox-polymers were synthesized by thermal polymerization of mono- and disubstituted quinoid derivatives of allylamine in the presence of elementary sulphur. Under the sulphur content in spatially linked samples discussed on reaction course, influence of conditions of synthesis on structure and properties of formed oxidation-reduction polymers.

INTRODUCTION:
Allyl polymers, owing to their improved physical and electric properties, high hemo- and thermal stability, cause a great interest of researchers [1-3]. However, initial monomers, including allylamine, possess low reactionary ability in polymerization reactions. Sufficiently severe conditions are necessary: high temperature (above 300-400°C), high pressure, γ-radiation. It limits their application.

It is known that introduction of electron acceptor substitutes in their structure essentially raises ability of monomers to polymerization [4]. We as such compounds have used 1,4-benzoquinone. The quinone-hydroquinone system is the most known and well studied oxidation-reduction system, and is widely used for the synthesis of redox-polymers [5].

MATERIALS AND METHODS:
Monomers – mono- (AA-Q) and disubstituted (AA-Q-AA) derivatives of allylamine (AA) and 1,4-benzoquinone (Q) were synthesized by methods [6].

Thermal polymerization of monomers was carried out in ampoules in the range of temperatures 160-220 °C and duration of process – 7 h. Content of sulphur in reaction medium was 5-50% from the monomer mass. Yield of gel-fraction was determined by the method of extraction in Sohxlet apparatus. Samples of polymers were washed from unreacted monomers and sulphur by mixture of dimethylformamide and acetone (1:1) [7].

Thermal stability of allyl redox-polymers linear and reticular structure was studied by the method of thermogravimetric analysis (TGA) on the air at the interval of temperatures 20-400 °C with constant velocity of heating 4°C/min.

Stability linear and reticular redox-polymers to thermal hydrolysis was determined by the way of their boiling in water for a different time by [8] with subsequent control of static exchange (SEC) and oxidation-reduction (ORC) capacity.

RESULTS AND DISCUSSION:

Studying of polymerization of monomers on the basis of and 1,4-Q has shown that for them is equally successful either radical [6,7] or, cation [9] initiation. Thus formed linear and weakly branched redox-polymers. However, in many cases it is more preferable to use spatially linked polymers.

In this connection we investigate thermal polymerization of AA-Q and AA-Q-AA in the presence of sulphur. The choice of sulphur as the linking agent is caused by two reasons: first, necessity of its recycling caused by annual growth of dumps of sulphur in connection with rapid development of the oil-extracting industry in Republic of Kazakhstan. Secondly, introduction of thyol groups in addition to quinoid provides alongside with oxidation-reduction properties an ability to selective extraction of ions of silver [5].

Thermal polymerization of monomers AA-Q and AA-Q-AA is investigated in the presence of sulphur of a deposit of Zhanazhol of the Aktyubinsk area (Fig. 1, curve 1), elementary sulphur (curve 2), UOS "Tengizshevroil" (curve 3).
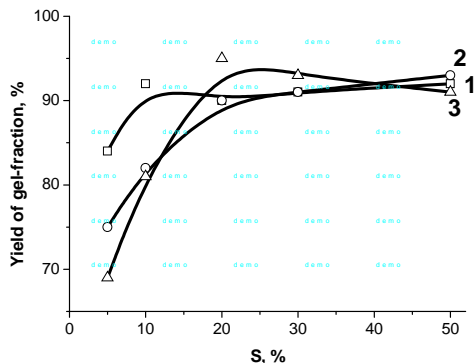

Fig. 1 Influence of quantity of sulphur on the yield of gel-fraction at - - polymerization (200^0 , 5 h) (1 – Zhanazhol, 2 – elemental sulphur, 3 – "Tengizshevroil")

Atoms of sulphur possess high ability to incorporate with each other with formation of ring or chain figures. If elementary sulphur is presented basically in a kind of octahedron cycles S_8 as a part of a product of sulphur cleaning the oil and gas raw materials alongside with forms S_8, S_6 there are active low-molecular forms S_{2-}, S_{3-}, S_{4-}, S_{5-} - forms [10]. But apparently from figure 1, these distinctions do not render essential influence on character of the received curves and a gel-fraction yield at polymerization of disubstituted quinoid derivative of allylamine. Reaction of linking in the course of monomer polymerization at temperature of 200° and durations of heating 5 h proceeds on the maximum depth equal to 91-93 %, in the presence of 10 % of Zhanazhol

sulphur and 20 % of elementary sulphur and Open Society "Tengizshevroil" sulphur. Thus, the sulphur taken from oil deposits, despite their various modifications, can be used with success in linking processes, in processes of sulphuric vulcanization of macromolecules.

The highest content of sulphur in polymerization products is observed at 200° (Fig. 2).
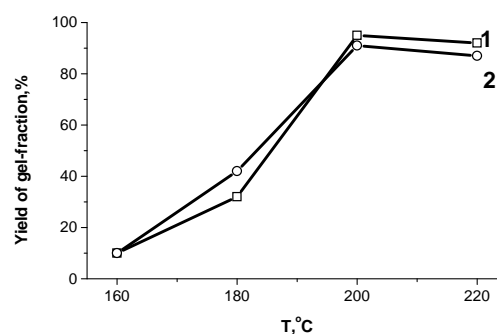

Fig. 2 Influence of temperature of polymerization of monomers - (1) and - - (2) on the yield of gel-fraction in the presence of 10% S (5 h)

In the presence of sulphur in an initial monomeric mix the gel-fraction yield (to 93-96 %) essentially raises. Depending on its content by results of the element analysis into structure of polymers enters to 26 % of sulphur. For lack of sulphur in an initial mix of reagents the yield of gel-fraction for AA-Q and AA-Q-AA reaches only 56 and 64 % accordingly (Table 1).

Table 1. An yield of gel-fraction and the content of the connected sulphur in the reticular redox-polymers obtained by thermal polymerization of monomers AA-Q and AA-Q-AA at various quantities of sulphur in initial reaction medium (= 200° , 5h)

Monomer	S, %		Yield of gel-fraction, %
	In the initial Mixture	In gel-fraction	
-Q	0	0	56,2
	5	4,3	65,4
	20	12,3	96,1
	50	26,6	95,3
AA-Q-AA	0	0	64,1
	5	4,7	75,3
	20	14,9	90,1
	50	25,8	93,0

According to data [11] radical process here takes place. Under the influence of radicals there is a disclosing of octahedron rings of elementary sulphur. Formed instable intermediate compounds break up with allocation of biradicals of sulphurs containing variable quantity of its atoms $\cdot S_{8-}$. The last also form cross-section connections in the course of polymerization of monomers. And at the

first stages polysulphidic compound are formed which then rearrange in groups with the smaller content of atoms of sulphur. On the other hand, there is an opinion [12] that with the same probability can proceed the ionic processes. The mechanism of these transformations demands special researches.

One of the basic characteristics of redox-polymers is the oxidation-reduction capacity [5]. Presence in allyl redox-polymers of amino groups where the atom of nitrogen has not divided pair of electrons, assumes ability to a complex formation. In this compounds important parameter at use of redox-ionites in practice for extraction of ions of various metals is sorption capacity which is defined by static exchange capacity (SEC) (Table 2). Apparently, the received reticular polymers have lower values ORC (2,7-3,0 mg-equ/g), than their linear analogs

Table 2. Sorption and oxidation-reduction capacity of polymers on the basis of quinoid derivatives of allylamine of linear and reticular structure

Polymer	SEC, mg-equ/g	ORC, mg-equ/g	EC_{Ag}, mg-equ/g
-(-AA-X-)n-	7,8	3,5	-
-(-AA-X-AA)n-	7,3	3,2	-
-(-AA-X-)n-:S	7,7	3,8	6,5
-(-AA-X-AA)n-:S	6,9	4,2	5,8

(3,2-3,5 mg-equ/g). However, the method of synthesis of sulphur containing redoxites in one stage is convenient in the technological relation as necessity of preliminary synthesis of macromolecules and their subsequent linking by sulphur disappears. Besides such polymers are perspective for extraction of ions of silver. Allyl polymers do not possess such ability.

The morphology of surfaces of linear and reticular redox-polymers on the basis of AA considerably differs. The surface of linear polymers on the basis of monoreplaced derivative (Fig. 3 , b) consists of layers, more tightly adjoining to each other, than in polymers from disubstituted monomer.
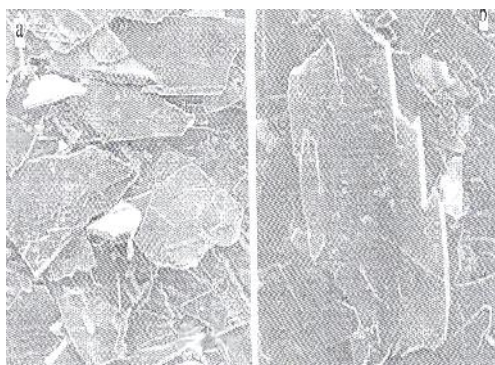

Fig.3 Electronic microphotograph of linear redox-polymer on the basis of AA-Q (a) and Q-AA-Q (b)

Synthesis of the spatially-structured redox- polymers by thermal polymerization of monomers in the presence of sulphur leads to formation of surfaces of other kind. The surface of reticular polymer on the basis of monoreplaced derivative (Fig. 4a) represents a set of craters of various diameter. At use for synthesis of reticular redox-polymer of disubstituted derivative its surface sharply changes (Fig. 4b).
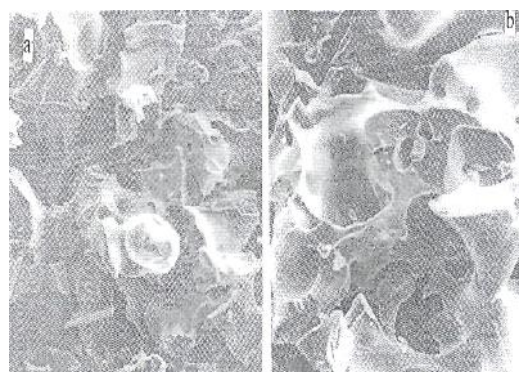

Fig.4 Electronic microphotograph of reticular redox-polymer on the basis of AA-Q (a) and Q-AA-Q (b)

Change of structure of monomers at their thermal polymerization with sulphur is accurately traced at comparison of their IR-spectra. Connections -S and S-S not so easy to identify, as band of absorption corresponding to them are exclusively little intensive and position of bands very variable [13]. However, occurrence on IR-spectra of redox- polymers a wide absorption band in the field of 400-700 sm^{-1} gives the grounds to assume that at their structure of connection – S-S - (400-500 sm^{-1}) and - -S- (600-700 sm^{-1}) are present.

The power system concerns perspective scopes of oxidation-reduction polymers. With their help it is possible to delete the oxygen dissolved in water causing corrosion of equipment of coppers. Thus rigid demands are made to them concerning their thermal stability. High-molecular compounds on the basis of allylic compounds possess a number of the valuable properties one of which is thermal stability.

Processes of destruction of ionites in a dry condition allow to estimate appreciably thermal stability of a matrix and functional groups, and also to define reference temperatures of destruction of macromolecules. Results of the thermo gravimetric analysis linear and linked allyl oxidation-reduction polymers are presented in Fig. 5. Thermal destruction of homopolymers, received on the basis of mono- and disubstituted allyl derivatives of quinone, proceeds almost equally. Thermal stability -[-   -Q-]n- is insignificantly higher, than at -[-   -Q-   -]n-. Their

reference temperature of destruction is identical, their weight starts to decrease at 170-180° . Losses for -[- -Q-]$_n$- and -[- -Q- -]$_n$- make at 200 ° accordingly nearby 1,0 and 1,2 %, at 300° - 20,5 and 22,0 %, at 400° - 28,8 and 29,2 %.
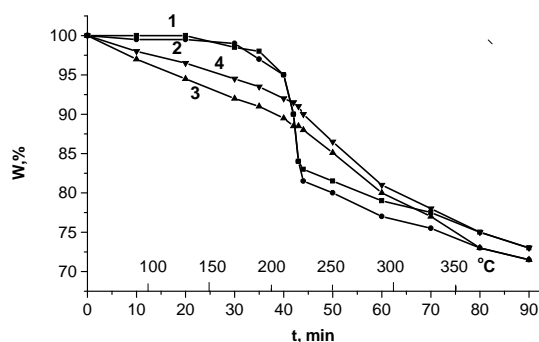

Fig. 5 Curves of mass loss of redox-polymers of linear (1, 2) and reticular (3, 4) structure on the basis of -Q (1, 3) and -Q- (2, 4)

Apparently from figure, higher thermal stability possesses redox-polymer reticular structure on the basis of disubstituted monomer (-[- -Q- -]$_n$-:S). Losses of weight for (-[- -Q-]$_n$-:S) and (-[- -Q- -]$_n$-:S) make accordingly at 200° - 9,5 and 7,0 %, 300° -21,0 and 19,5 %, 400° - 30,8 and 28,4 %. Thus, in the beginning on curves monotonous reduction of weight of samples to temperatures 230° for (-[- -Q-]$_n$-:S) and 220° for (-[- -Q- -]$_n$-:S) is observed. Then speed of loss of weight increases, and is sharper for the second redox-polymer, and after 300° is again slowed down. At heating on air at 300-400° losses of weight of redox-polymers of linear and reticular structure are almost identical. From what it is possible to conclude that thermal destruction of their matrixes proceeds similarly owing to what they do not differ on the thermal stability.

Research of processes of thermal hydrolysis allows to estimate stability of properties of ionites more precisely. The obtained data plays an important role and for practical application of redox-polymers as them use for clearing of water solutions. Results of thermal hydrolysis of the linear and linked redox-polymers are resulted in Table 3.

Table 3. Thermal stability of redox- polymer linear and reticular structure in water

Polymer	6 h		24 h		36 h	
	SEC,%	ORC,%	SEC,%	ORC,%	SEC,%,	ORC,%
-(-)$_n$-	95,9	94,7	89,6	80,0	87,5	68,5
-(- -AA)$_n$-	95,4	90,8	90,0	82,4	87,8	79,6
-(- -:S)$_n$-	98,3	97,2	92,0	89,5	90,0	84,2
-(- -AA-:S)$_n$-	97,2	98,8	92,2	90,5	89,5	90,5

As data Table 3 shows, to the SEC and ORC all investigated samples with increase of duration of a boiling in water decrease. Losses to the SEC of the linear redox-polymers received on the basis of both mono- and disubstituted allylic derivatives of quinones, are identical. Similar changes are observed also at redoxites reticular structure. However ORC at a boiling in water during 36 h remains as at linear, so the linked samples synthesized on the basis of disubstituted allylic monomer is better. Stability of reticular structured polymers to thermohydrolysis is higher than at linear as the loss of SEC and ORC linked samples are less.

It is shown that the structure of redoxites does not influence on their thermal stability at heating on air above 300° and make essential impact on their stability to thermal hydrolysis. At boiling in water thermostability of reticular structured polymers are higher than linear.

CONCLUSIONS:
Thus, synthesis, structure and properties of sulphurcontaining quinoid redox- polymers, obtained by thermal polymerization of allylic monomers in the presence of elementary sulphur and sulphur of various deposits of Kazakhstan, were studied. It was shown that sulphur can be effectively used for structurization of macromolecules of allylamine in the course of their formation at radical initiation of quinoid derivatives of allylamine.

ABBREVIATIONS:
AA allylamine
AA-Q monosubstituted derivatives of allylamine
AA-Q-AA disubstituted derivatives of allylamine
Q benzoquinone
IR- spectra infra red spectra
ORC oxidation-reduction capacity
SEC static exchange capacity
TGA thermo gravimetric analysis

REFERENCES:

1. Timofeeva LM. Radical polymerization of secondary and tertiary diallilamines and property of polymers on their basis: abstract dis... Doctors of Chemistry. Moscow. 2011: 48 (In Russian).
2. Fattakhov MN, Ismailov RR, Shakiryanov ED, Sivergin YuM, Usmanov SM. Modeling of dynamics of development of the three-dimensional polymeric structures of a diallylizoftalat. The bull . of the Nizhny Novgorod university of N.I. Lobachevsky. 2; 2011: 141–147 (In Russian).
3. Volodina VI, rasova I and Spasskii SS, Uspechi chimii. 39; 1970:276 (In Russian).
4. banov V , Zubov VP and Semchikov YuD. mplex-radikal polymerization. Chimia. Moscow. 1987 (In Russian).
5. Cassidy HG, KunKA. Oxdation-reduction polymers (Redox Polymers). Interscience Publishers. New-York. 1965 (In Russian).
6. rgozhin EE, ukhitdinova BA, Shoinbekova SA, Nuranbaeva BN, Moldagazieva ZhI, Zhunusova GN. New oxidation-reduction monomers and polymers on the basis of monoethanolamine vinyl ethers, allylamine and some quinones. Reactive and Functional Polymers. 65; 2005:101-113.
7. Mukhitdinova BA, Ergozhin EE, Nikitina AI, Razuvaeva NI. Study of quinoid derivatives of allylamine polymerization. Asian J. Res. Chem. 9; 2011:1366-1370.
8. Tulupov PE, Konovalova OT, Gerasimova VV in "Sorption and chromatography". Nauka. Moscow. 1979 (In Russian).
9. rgozhin EE, ukhitdinova BA, Shoinbekova SA, Nikitina AI. Activity mono - and disubstituted derivatives of 1,4-quinone and allylamine in cationic polymerization. Zhurnal prikladnoi chimii. 80; 2007:1037 (In Russian) .
10. Suleimenov JT, Ospanova MSh, Markonrenkov YuA. Efficiency of stabilization of polymeric modification of sulfur. Chem. J. Kazakhstan. 2; 2006:105 (In Russian) .
11. Alliger G, Ijetuna IM. Vulcanization of elastomers. Chimia. Moscow. 1967 (In Russian).
12. Dogadkin BA, Shershnev VA. Uspechi chimii. Curing of rubbers in the presence of organic accelerators. 30; 1961:1013 (In Russian).
13. Bellamy L. Infrared spectra of complicated molecules. IL. Moscow.1963 (In Russian).

REVIEW ARTICLE

Review on Guideline on Elemental Impurities

Poonam R. Songire[1], Prof. Smita Aher[2]*, Prof. Dipti Phadtare[2] Dr. Saudagar R. B.[2]
[1]Department of Quality Assurance Technique, R.G. Sapkal college of Pharmacy, Anjaneri, Nashik, Maharashtra, India.
[2]Department of Pharmaceutical Chemistry, R. G. Sapkal College of Pharmacy, Anjaneri, Nashik, Maharashtra, India.
*Corresponding Author E-mail: **poonamsongire1@gmail.com**

ABSTRACT:
Abstract are related to the elemental impurities it included identification, structural elucidation and quantitative determination of impurities. It included According to ICH guidelines, Impurities associated with APIs are classified into the categories. In elemental impurities Four-step process to assess and control elemental impurities in the drug product. Identification of impurities is done by variety of Chromatographic and Spectroscopic techniques, either alone or in combination with other techniques. These impurities are control with strategy.

KEYWORDS: Elemental impurities, Types of impurities, Control strategy.

INTRODUCTION OF ICH Q3D:

The introduction of ICH Q3D is listed 24 elements that need to be evaluated by drug manufacturers, including mercury, lead, cadmium and arsenic. It included heavy metals in elemental impurities. Sources are elemental impurities are form residual catalysts added in synthesis, arising from processing equipment, presents in components of the drug product. Elemental classification is included four classes. The introduction of ICH Q3D (1) is one of the most complex changes in regulations pertaining to impurities seen by the pharmaceutical industry. While the guideline is ultimately intended to focus on final drug product quality, the actual risk assessment will touch all facets of the manufacture of a drug product. The guideline introduces toxicologically relevant permitted daily exposure (PDE) limits to individual elements replacing non-specific 19th century wet chemical "heavy metal" limit tests.

ICH Q3D advocates the use of a risk-based approach to assessing the potential for presence of elemental impurities in drug products. The process of executing and documenting the risk assessment is a major challenge, primarily as a result of a limited global understanding about how to assess or quantify the risk associated with factors such as water, container-closure systems, and recipients[1].

SOURCES AND TYPES OF IMPURITIES:-

According to ICH guidelines, Impurities associated with APIs are classified into the following categories:

- Organic impurities (Process and Drug related)
- Inorganic impurities
- Reagents, ligands and catalysts
- Heavy metals
- Residual solvent

1) Organic impurities:

Organic impurities may arise during the manufacturing process and/or storage of the drug substance. They may be identified or unidentified, volatile or non-volatile including starting materials, by-products, intermediates, degradation products, reagents, ligands and catalysts.

226

Starting materials or intermediates are the most common impurities found in every API unless a proper care is taken in every step involved in throughout the multi-step synthesis.

2) Inorganic impurities:

Inorganic impurities may also arrive from manufacturing processes used for bulk drugs. They are normally known and identified.

3) Reagents, ligands and catalysts-

The chances of presence of these impurities are rare. However, in some processes, these could create a problem unless the manufacturer takes proper care during production.

4) Heavy metals-

The main sources of heavy metals are the water used in the processes and the reactors (if stainless steel reactors are used), where acidification or acid hydrolysis takes place. These impurities of heavy metals can easily be avoided using demineralized water and glass-linked reactors.

5) Residual solvents [2]

Residual solvents are organic or inorganic liquids used during the manufacturing process. It is very difficult to remove these solvents completely by the workup process.

6) Environment related impurities:

Due to exposures to adverse temperatures (e.g. Vitamins as drug substances are very heat-sensitive and degradation frequently leads to loss of potency in vitamin products, especially in liquid formulations).

Due to exposure of light specially UV light (e.g. Ergometrine as well as methyl ergometrine is unstable under tropical conditions such as light and heat).

Humidity (Humidity is considered Humidity (Humidity is considered detrimental for hygroscopic products e.g. Aspirin and Ranitidine).

ELEMENTAL CLASSIFICATION [3]

Classification	Description	Include in Risk Assessment
Class 1	Significantly toxic across all routes of administration	Yes
Class 2	Toxic to a greater or lesser extent based on route of Administration	Class 2A – Yes Class 2B – Yes only if intentionally added
Class 3	Impurities with relatively low toxicity (high PDEs) by the oral route of administration but require consideration in the risk assessment for other routes of administration	Dependent upon route of Administration
Class 4	Elemental impurities have been evaluated but for which a PDE has not been established due to their low inherent toxicity and/or regional regulations	No

Process to assess and control elemental impurities [4]:-

Four-step process to assess and control elemental impurities in the drug product
1. Identify: Identify known and potential sources of elemental impurities that may find their way into the drug product.
2. Analyze: Determine the probability of observance of a particular elemental impurity in the drug product.
3. Evaluate: Compare the observed or predicted levels of elemental impurities with the established PDE.
4. Control: Document and implement a control strategy to limit elemental impurities in the drug product.

SAFETY ASSESSMENT OF POTENTIAL ELEMENTAL IMPURITIES:-

1. Principles of the Safety Assessment of Elemental Impurities for Oral, Parenteral [5] and Inhalation Routes of Administration

The factors considered in the safety assessment for establishing the PDE are listed below in approximate order of relevance:
- The likely oxidation state of the element in the drug product;
- Human exposure and safety data when it provided applicable information;
- The most relevant animal study;
- Route of administration;
- The relevant endpoint(s).

In the absence of data and/or where data are available but not considered sufficient for a safety assessment for the parenteral and or inhalation route of administration, modifying factors based on oral bioavailability were used to derive the PDE from the oral PDE:

- Oral bioavailability <1%: divide by a modifying factor of 100;
- Oral bioavailability 1% and <50%: divide by a modifying factor of 10;
- Oral bioavailability 50% and <90%: divide by a modifying factor of 2; and
- Oral bioavailability 90%: divide by a modifying factor of 1.

Where oral bioavailability data or occupational inhalation exposure limits were not available, a calculated PDE was used based on the oral PDE divided by a modifying factor of 100.[6]

2. Other Routes of Administration PDEs were established for oral, parenteral and inhalation routes of administration:-

- Based on a scientific evaluation, the parenteral and inhalation PDEs may be a more appropriate starting point.
- Assess if the elemental impurity is expected to have local effects when administered by the intended route of administration:

Guideline for Elemental Impurities:-
1. If local effects are expected, assess whether a modification to an established PDE is necessary.
2. Consider the doses/exposures at which these effects can be expected relative to the adverse effect that was used to set an established PDE.
3. If local effects are not expected, no adjustment to an established PDE is necessary.
4 If available, evaluate the bioavailability of the element via the intended route of administration and compare this to the bioavailability of the element by the route with an established PDE:
5. When a difference is observed, a correction factor may be applied to an established PDE.
For example, when no local effects are expected, if the oral bioavailability of an element is 50% and the bioavailability of an element by the intended route is 10%, a correction factor of 5 may be applied.
6.If a PDE proposed for the new route is increased relative to an established PDE, quality attributes may need to be considered.

Justification for Elemental Impurity [7, 8]:-
Levels of elemental impurities higher than an established PDE may be acceptable in certain cases. These cases could include, but are not limited to, the following situations:

- Intermittent dosing;
- Short term dosing (i.e., 30 days or less);
- Specific indications (e.g., life-threatening, unmet medical needs, rare diseases).

RISK ASSESSMENT:
The evaluation of the potential risk posed by elemental impurities within a formulated drug product requires a holistic approach taking into account all potential sources of elemental impurities. **Figure 1** illustrates potential sources that should be considered in such an evaluation.
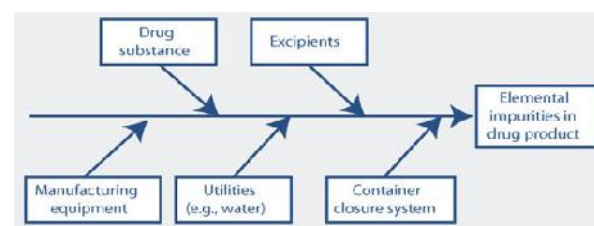

Figure 1: Sources of elemental impurities in finished drug products.

1) Drug substance
As presented in Figure 1, the drug substance is a key component that can contribute elemental impurities to the finished drug product. The risk of inclusion of elemental impurities from a drug substance, therefore, needs to be considered when conducting a drug product risk assessment. Control of the elemental impurity content of a drug substance can be assured through a thorough understanding of the manufacturing process including equipment selection, equipment qualification, GMP processes, packaging components, and the selection and application of appropriate control strategies.

A principal responsibility for any drug-substance manufacturer is to develop a strategy to ensure effective control of the levels of elemental impurities in the finished drug substance. An approach based on assessing and controlling potential sources of elemental impurities, coupled with focused, limited testing, is preferable to exhaustive testing on the finished drug substance. A scientific, risk-based approach combined with knowledge and control of the key sources of elemental impurities in the drug-substance manufacturing process such as catalysts, provides an efficient and comprehensive elemental impurity control strategy for finished drug substances.

Figure 2 shows potential sources of elemental impurities in the drug substance manufacturing process. Of the sources highlighted, the greatest risk comes from intentionally added metals (e.g., metal catalysts used in the process). Manufacturing equipment, processing aids, inorganic reagents, water, solvents, and other organic materials are less likely to serve as major contributors of elemental impurities in the finished drug substance, but do require consideration.
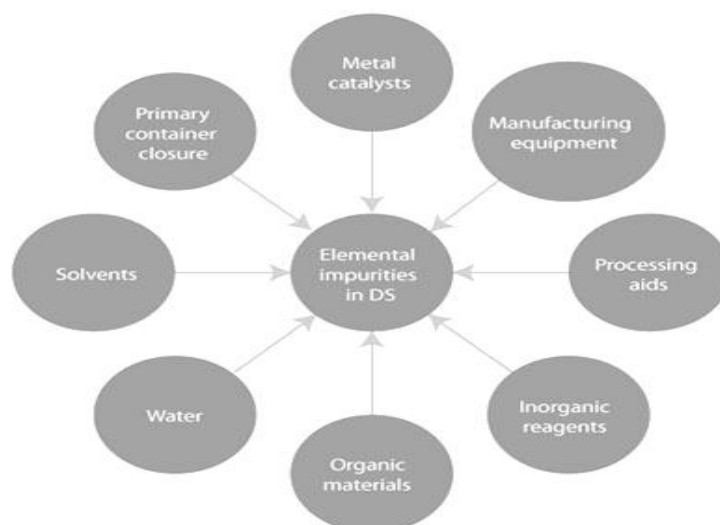
Figure 2: Primary sources of elemental impurities in drug substances.

2) Metal catalysts [9]

Metal catalysts such as palladium and platinum are often used in the drug substances manufacturing process and can therefore be present at low levels in the finished drug substance. The synthetic route should be reviewed for intentionally added metals, and data from purging studies, including any Supportive testing of appropriate isolated intermediates, should be used in the design of an appropriate control strategy. The ability to remove the catalyst (purge capacity) will be influenced by catalyst loading and the nature of the catalyst used in the process (Homogeneous vs. Heterogeneous catalysts). Heterogeneous catalysts, such as palladium on carbon, are often easily Removed from reaction mixtures by filtration, and therefore, the risk of carryover of elemental impurities into the drug substance are typically low. Even in cases where metal catalysts are used in the final stages of the process, good historical data and/or understanding of carry-over may permit reduced testing schemes. When considering the other Potential sources highlighted in Figure 2, it is recommended to focus primarily on the manufacturing steps that occurs after the formation of the final intermediate. Washes, crystallizations, phase separations, Chromatography, distillations, and processing Aids/scavengers aid in purging of elemental impurities and, therefore, reduce the risk of carryover into the finished drug substance from stages earlier in the upstream process. Areas for further Consideration include manufacturing equipment, processing aids/inorganic Reagents, solvents, water, and packaging.

3) Manufacturing equipment.

In general, GMPs, including equipment compatibility assessment and qualification, are sufficient to ensure that significant levels of elemental impurities are not leached from manufacturing equipment into the drug substance. Hastily, stainless steel, and glass are the most commonly used materials of construction for drug substance manufacturing equipment, due to their superior chemical resistance. Nickel, cobalt, vanadium, molybdenum, chromium, and copper are key elements in some Hastelloy and stainless-steel alloys. Under extreme/corrosive reaction conditions, such as high temperature and low/high pH, these elements could have the potential to leach from manufacturing equipment. In such cases, it may be necessary to supplement standard GMP equipment compatibility assessments with specific studies to assess the elemental impurity-leaching propensity from manufacturing equipment due to corrosive reaction conditions.

Particle size reduction is discussed in the Drug Product Manufacture section.

4) Inorganic reagents.

Processing aids such as charcoal, silica, celite, and Draco, and inorganic reagents such as sodium chloride, magnesium sulfate, and sodium sulfate, are often used in drug-substance manufacturing processes and may be used in significant quantities. Depending on their specific composition, inorganic reagents should be considered within the risk assessment, especially when ICH Q3D elements are integral to the formula.

Therefore, the risk assessment should primarily focus on processing aids and inorganic reagents used late in the drug substance manufacturing process, and/or where aggressive reaction conditions exist (e.g., extreme pH/high temperatures for prolonged times).

5) Solvents [2].

Most solvents used in the manufacture of drug substances, particularly those listed in ICH Q3C, Impurities: Guideline for Residual Solvents (2) Class 3, are unlikely to contribute elemental impurities to the finished drug substance. The majority of solvents are purified by distillation and few involve the direct use of metal catalysts in their manufacture; hence they are considered a low risk source of elemental impurities. In the event that solvents have not been purified by distillation, especially if a catalyst in used in their manufacture, further evaluation in the risk assessment should be considered.

6) Packaging.

Packaging is discussed in the section Container-closure Systems (CSS) as a Potential Source of Elemental Impurities in Finished Drug Product.

7) Evaluation option limits.[10]

It must be recognized that, from a compliance perspective, the limits for elemental impurities in ICH Q3D apply only to the drug product. To ensure effective control of the level of elemental impurities in the drug substance a number of options are available:

- The ICH Q3D option 1 concentration limits assume a maximum daily drug product intake of 10 g/day. Drug substances that meet option 1 concentration limits can be used at any dose in the drug product.
- ICH Q3D option 2 concentration limits are calculated specifically based on the actual daily drug product intake (and composition) and may provide higher concentration limits than option 1 (if the maximum daily intake of drug product is <10g).

The acceptable level of elemental impurities in a drug substance may be defined and agreed upon in a suitable quality agreement between the drug substance manufacturer and the drug product manufacturer.

CONTROL OF ELEMENTAL IMPURITIES:-

- Control of elemental impurities is one part of the overall control strategy for a drug product that assures that elemental impurities do not exceed the PDEs.
- When the level of an elemental impurity may exceed the control threshold, additional measures should be implemented to assure that the level does not exceed the PDE.
- Approaches that an applicant can pursue include but are not limited to:

- Modification of the steps in the manufacturing process that result in the reduction of elemental impurities below the control threshold through specific or non-specific purification.

- Implementation of in-process or upstream controls, designed to limit the concentration of the elemental impurity below the control threshold in the drug product;

- Establishment of specification limits for excipients or materials (e.g., synthetic intermediates);

- Establishment of specification limits for the drug substance;
- Establishment of specification limits for the drug product;

- Selection of appropriate container closure systems.
- Periodic testing may be applied to elemental impurities according to the principles described in ICH Q6A.
- The information on the control of elemental impurities that is provided in a regulatory submission includes, but is not limited to, a summary of the risk assessment, appropriate data as necessary, and a description of the controls established to limit elemental impurities.

CONTROL STRATEGY:

A drug-product risk assessment can use prior knowledge of the input materials to demonstrate that the risk of significant elemental impurity levels is low across multiple batches. When the risk assessment concludes that elemental impurities are below 30% PDE, it should be acceptable to rely on the quality system to maintain the control of the process and the existing use of standard cGMPs as a control strategy of the drug product, without requiring any additional element-specific testing on each batch of product[11].

Other factors to consider could include:

- Security of external supply chain along with a quality history (e.g., audit history, levels of complaints, recalls, etc.) for each vendor
- Control of vendor elemental impurity specifications and elemental impurity reporting on ingredient certificates of analysis
- Security of internal supply chain.

It is anticipated that a properly executed and documented elemental impurity risk assessment for the majority of drug products may justify the use of standard cGMP as being a sufficient control strategy to ensure levels of elemental impurities meet the levels

defined in ICH Q3D, without the need for additional testing.

Where the drug product elemental impurity risk assessment identifies the need for additional elemental impurity control, it is crucial to first understand the potential source of the elemental impurity(s). Once the source is known, appropriate controls, in addition to cGMP, can be applied. The flow chart in can be followed to help determine when additional controls are required and what those controls may look like.
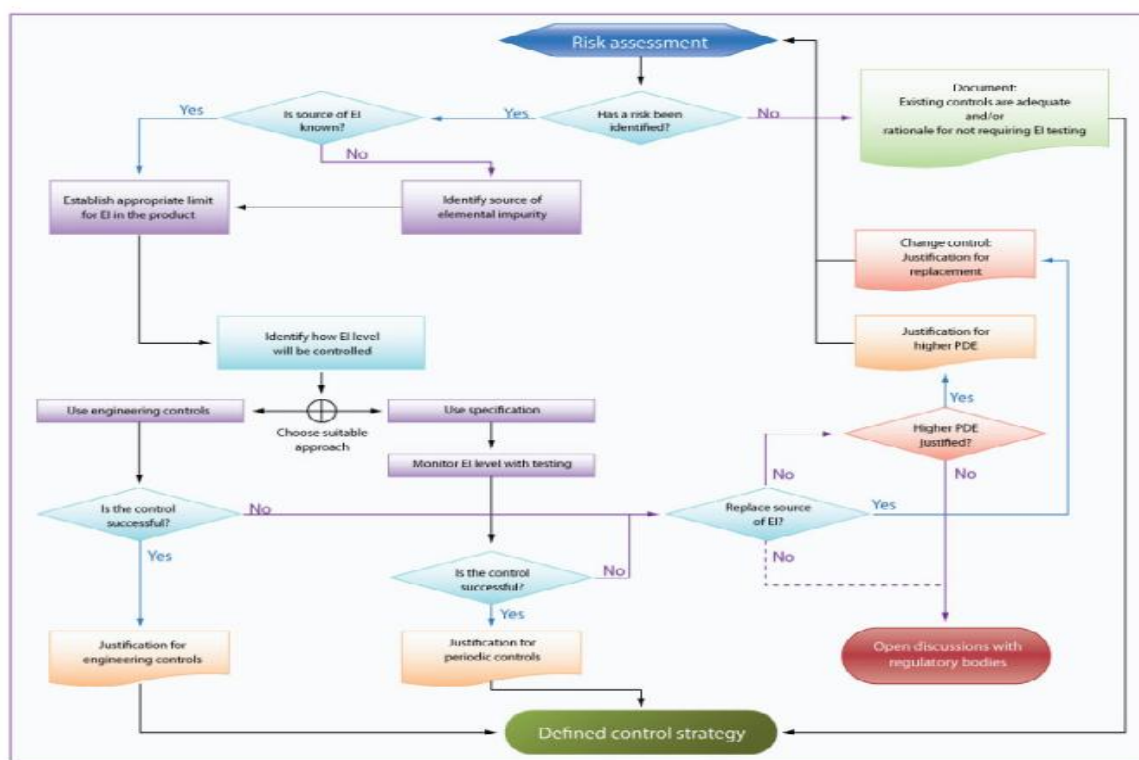

Fig: - Elemental impurity control strategy

CONCLUSION:
The implementation of the ICH Q3D guideline can be adequately achieved through using an appropriate risk-based process combined with existing GMP standards. A risk assessment should be performed to identify any elemental impurities that may potentially be present at significant levels in the drug product. Such an assessment is then used to define an appropriate control strategy. ICH Q3D allows the option that the scope and extent of quality control testing may be reduced, or even eliminated provided there is adequate control. In many cases, this can be successfully achieved through the use of appropriate GMP controls both in terms of input materials and manufacturing processes, limiting testing to those areas clearly identified as a substantive risk.

REFERENCES:
1. Q3D Guideline for Elemental Impurities, **International Conference Harmonization**,.(2014)
2. Q3C Impurities: Guideline for Residual Solvents, **International Conference Harmonization**, (2011).
3. Haxel GB, Hedrick JB, Orris GJ. Rare earth elements-critical resources for high technology. **US Geological Survey** 2005; Fact Sheet 087-02.
4. Elemental Impurities-Procedures, **United State Pharmacopoeia**, General Chapter 233
5. Holliday MA, Segar WE. The maintenance need for water in parenteral fluid therapy. Pediatrics 1957; 19:823-32
6. Ball D, Blanchard J, Jacobson-Kram D, McClellan R, McGovern T, Norwood DL et al. Development of safety qualification thresholds and their use in orally inhaled and nasal drug product evaluation. **Toxicology Sci** 2007; 97(2):226-36.
7. IPCS. Principles and methods for the risk assessment of chemicals in food, chapter 5: dose-response assessment and derivation of health based guidance values. Environmental Health

Criteria 240. **International Programmed on Chemical Safety**. World Health Organization, Geneva. 2009.

8. US EPA. 0410 Boron and Compounds. **Integrated Risk Management System (IRIS)**. 2004

9. EMEA, Guideline on the Specification Limits for Residues of Metal Catalysts or Metal Reagents, EMEA/CHMP/ SWP/4446/2000 (2008)

10. S. Ahuja, Marcel Dekker, **Impurities Evaluation of Pharmaceuticals**,, Inc. New York, 2006.

11. D. Jenke et al**, PDA J Pharma Sci and Tech**, 67, 354-375 (2013).